

Université du Québec

Institut National de la Recherche Scientifique

Énergie Matériaux Télécommunications

Cramer-Rao Lower Bounds for Channel Parameters Estimation over Turbo-Coded Wireless Transmissions

Préparé par

Achraf Methenni

Mémoire présenté pour l'obtention du grade de Maître ès Sciences (M.Sc.) en

Télécommunications

Examinateur Externe

Prof. Fabrice Labeau

McGill University

Examinateur Interne et Président du jury Prof. Nahi Kandil

Prof. Nahi Kandil
jury *UQAT*

Directeur de Recherche Prof. Sofiène Affes

INRS-ÉMT

To my parents

To Sadok, Imen and Haythem

To Zizou, Bibou, Ahmed and Yassine

Acknowledgements

I wish to thank Prof. Sofiène Affes for giving me the opportunity to work in his team, and for guiding me throughout my MSc program. His remarks as well as his pertinent criticism led me to the right path.

I want also to thank Mr. Faouzi Bellili for all his efforts, for being there for me, providing me with valuable advices and providing the perfect example for me for my research career. A special thanks to the external and internal jury members, Prof. Fabrice Labeau from McGill University and Prof. Nahi Kandil from UQAT and adjunct professor at INRS-EMT who have kindly accepted to assess my MSc thesis. I want to express my thanks and gratitude to all my family, for their patience, and for all their encouragements.

Finally, I want to thank all my colleagues and all the staff at INRS for providing a perfect environment, and for making me feel as if I was surrounded by my family members...

Table des matières

Résumé	2
1 Introduction	12
2 System Model	19
3 Derivation of the Log-Likelihood Function (LLF)	24
3.1 LLF for BPSK and MSK signals :	27
3.2 LLF for QPSK signals :	28
3.3 LLF for square-QAM signals :	30
4 Derivation of the CRLB Analytical Expressions	45
4.1 CRLB for coded SNR estimation [43]	45
4.2 CRLB for coded phase and CFO estimtion [44]	52

4.2.1	Empirical Evaluation of the CRLB	56
5	Simulation Results	60
5.1	SNR estimation	60
5.2	Phase and CFO estimation	64
6	Conclusion	70
	Conclusion	70

Table des figures

3.1	Construction of Gray-coded Square-QAM constellations	34
3.2	Construction of Gray-coded Square-QAM constellations	41
5.1	CA CRLBs for SNR estimation : 16-QAM, $K=207$	61
5.2	CA CRLBs for SNR estimation : BSK and MSK signals, $K=207$	62
5.3	CA CRLBs with different modulation orders : $K = 207$	63
5.4	CA CRLBs for different coding rates : 16-QAM, $K=207$	64
5.5	CRLB for the phase and CFO estimation using 16-QAM symbols with $K = 207$: (a) $\text{CRLB}(\phi)$, (b) $\text{CRLB}(\nu)$	66
5.6	CRLB for the phase and CFO estimation for different modulation orders with $K=207$ symbols : (a)- $\text{CRLB}(\phi)$,(b)- $\text{CRLB}(\nu)$	67
5.7	CRLB for the phase estimation for BPSK and MSK modulations $K=207$ sym- bols : $\text{CRLB}(\phi)$	68

5.8 CRLB for the phase : CRLB(ϕ) vs coding gain, for 16-QAM symbols, $K=207$. . 69

Résumé

La connaissance du rapport signal à bruit (RSB) est souvent nécessaire dans plusieurs applications en communications sans fil. En effet, plusieurs techniques d'optimisation des ressources radio sont, de nos jours, basées sur la connaissance *a priori* de ce paramètre clé. A titre d'exemple, les estimées du RSB sont typiquement utilisées en contrôle de puissance, modulations adaptatives et techniques de décodage [5, 16] :

- Contrôle de puissance : Avec la croissance rapide du nombre des utilisateurs, dans les réseaux de communications sans fil, le contrôle de puissance de transmission est devenu une procédure nécessaire pour minimiser l'interférence des utilisateurs. En effet, les émetteurs doivent ajuster leur puissance de transmission selon les conditions de propagation afin de garder l'interférence qui résulte de l'accès multiple au canal à un seuil permettant une qualité de service souhaitée.
- Ces conditions de propagation sont souvent jugées en termes du RSB des liaisons. En outre, si le RSB est suffisamment élevé (au dessus d'un seuil prédéfini), l'émetteur peut diminuer sa

puissance de transmission. Ceci permettra, entre autres, d'assurer une autonomie énergétique plus élevée au niveau des stations mobiles (qui ne sont la plupart du temps pas reliées au secteur).

- Dimensionnement des réseaux sans fil : La connaissance du RSB est aussi très utile pour les opérateurs en vue de dimensionner les réseaux sans fil à déployer. Elle permet, par exemple, en communications radio mobiles de déterminer à quel point la taille des cellules peut être réduite afin d'augmenter le facteur de réutilisation des fréquences. Ceci permet en l'occurrence d'augmenter la capacité totale du système.
- Handoff et allocation dynamique de ressources : Les procédures de handoff et allocation adaptative des ressources sont étroitement liées. Le handoff réfère à l'opération de faire passer un utilisateur de façon transparente d'une cellule à une autre. Ceci est dû essentiellement à la mobilité des utilisateurs dans le réseau. L'allocation dynamique de ressources consiste à optimiser l'exploitation des ressources du système selon les changements du trafic et du niveau d'interférence. Plusieurs de ces opérations reposent sur la qualité de la liaison qui est généralement caractérisée en fonction du RSB.
- Modulation adaptative : La technique de modulation adaptative consiste à changer, chez l'émetteur, le type et/ou l'ordre de la modulation afin d'augmenter le débit effectif. Ce chan-

gement dépend essentiellement du RSB de la liaison en question. En effet, si le niveau du RSB est élevé, l'ordre de la modulation utilisé peut être augmenté tout en gardant le même taux d'erreur binaire (TEB) de départ. Ceci permet, en outre, d'augmenter le débit de la liaison étant donné que les modulations d'ordre supérieur permettent de transmettre plus de “d'information binaire” par symbole. Cette stratégie est surtout utilisée en communications OFDM (orthogonal frequency division multiplxing) où la connaissance *a priori* du RSB joue un rôle primordial.

L'estimation du rapport signal sur bruit est aussi nécessaire dans plusieurs autres applications telles que le codage turbo, l'égalisation, les antennes adaptatives, etc., mais nous ne pouvons pas les détailler toutes, dans ce mémoire, par manque d'espace.

Dans ce contexte, malgré le fait que les premiers estimateurs du RSB remontent aux années 1960, ce problème a suscité une grande attention surtout durant ces deux dernières décennies. Ceci est dû, en partie, au grand succès des systèmes radio mobiles cellulaires et, en partie, aux avancées en microélectronique qui ont rendu réalisables des techniques d'estimation plus complexes.

Les estimateurs du RSB sont généralement classés sous deux grandes catégories : autodidactes et assistés. En estimation autodidacte, les symboles transmis sont supposés complètement in-

connus par le récepteur. L'estimation du RSB repose alors uniquement sur les statistiques du signal reçu. Les estimateurs qui appartiennent à cette catégorie sont appelés estimateurs NDA (non-data aided). Ils requièrent souvent un grand nombre d'échantillons reçus pour obtenir des estimées suffisamment précises du RSB. Les techniques NDA sont, par contre, plus appréciées en pratique parce qu'elles n'affectent pas le débit effectif du système. Elles permettent, en effet, une estimation en temps réel du paramètre en question et elles sont de ce fait aussi qualifiées d'estimateurs “in service”. Les méthodes assistées nécessitent, par contre, la connaissance *a priori* de la séquence transmise pour estimer le RSB. Elles sont connues en littérature sous le nom d'estimateurs DA (data-aided). Il y a, en fait, deux types de techniques DA :

- Techniques TxD A : ces techniques nécessitent l'introduction d'une séquence de symboles transmis qui est parfaitement connue par le récepteur. La fidélité de la séquence du message utilisée pour l'estimation est garantie par le fait même qu'une copie conforme de cette séquence est disponible à la réception. En pratique, de petites séquences de données connues (séquences pilotes) peuvent être insérées périodiquement dans un flux de données à transmettre.

Les procédures d'égalisation et de synchronisation utilisent aussi ce genre de séquences, dites aussi séquences d'apprentissage. L'utilisation de telles séquences pour l'estimation du RSB diminue le débit utile du système. Néanmoins, pour des systèmes utilisant déjà des séquences

pilotes pour la synchronisation ou l'égalisation, on peut utiliser ces mêmes séquences pour l'estimation du RSB sans aucune pénalité supplémentaire. Notez ici que, puisqu'une estimation TxD A ne peut être faite qu'en présence de la séquence pilote, l'utilisation de cette méthode n'est pas adéquate dans les cas où une estimation continue du RSB est exigée.

- Technique RxDA : Ces méthodes reposent sur l'utilisation des symboles détectés. Ces derniers remplacent alors la séquence des symboles pilotes pendant le processus d'estimation. Ces algorithmes sont aussi appelés DD (decision-directed). Ils souffrent des erreurs de détection et leurs performances sont alors inférieures à celles des estimateurs TxD A. Cependant, ils peuvent être utilisés dans le cas où une estimation continue du RSB est nécessaire. Ils sont alors qualifiés d'estimateurs “in service”, tout comme les estimateurs NDA, et ils n'affectent pas le débit du système.

Les approches non assistées ont l'avantage de ne pas affecter le débit global du système de communications (haute efficacité spectrale). Néanmoins, elles présentent une performance très pauvre dans le régime bas RSB, particulièrement pour des données de courte longueur. Pour remédier à ce problème en préservant l'efficacité spectrale, on a envisagé l'estimation codée pour améliorer la performance de l'estimation dans ces conditions difficiles. Dans ce contexte, les turbo codes [6-8] ont gagné considérablement l'attention des chercheurs durant les deux dernières

décennies grâce à leur capacité impresionnante à opérer près de la limite de Shannon, même dans des bas RSBs. Récemment, il a été montré que l'estimation du SNR peut être améliorée substantiellement en exploitant l'information a priori délivrée pendant le processus de décodage des données transmises. Dans les systèmes turbo-codés, par exemple, l'estimation codée peut profiter de l'information souple (comme de l'information à priori) obtenue du décodeur souple (entrée souple sortie souple). L'algorithme de décodage souple (dans le sens du minimum du taux d'erreur binaire) est l'algorithme du maximum à posteriori, connu aussi sous le nom de BCJR.

Cependant, l'implémentation de cet algorithme optimal requiert en elle-même la connaissance a priori du RSB. C'est pourquoi l'effet de l'erreur d'estimation du RSB sur la performance des systèmes turbo-codés a été le sujet de plusieurs études [16-18].

– Effet d'une erreur d'estimation du RSB sur la performance des turbo-codes :

Il a été trouvé, que dans le cas d'un système à modulation binaire (BPSK), la surestimation jusqu'à plusieurs dB est tolérable en termes de performances de décodage, tandis que la sous-estimation au-delà de 2 dB conduit à d'importantes erreurs de décodage. Dans le cas d'un code turbo combiné avec des schémas de modulation d'ordre supérieur, comme la modulation d'amplitude en quadrature (QAM), sa sensibilité à l'erreur d'estimation du RSB

s'est révélée être différente qu'avec BPSK. Le RSB estimé joue un rôle différent dans le calcul de métriques binaires pour différents schémas de modulation, et conduit donc à des performances de décodage différentes. Dans les systèmes modulés d'ordre élevé, la tolérance du turbo code à une erreur d'estimation du RSB est considérablement réduite, particulièrement à une surestimation [20].

D'autre part, la phase du canal et le résidu de la fréquence porteuse(RFP) sont considérés comme paramètres clés dont la connaissance peut être exploitée à la réception pour atteindre la meilleure performance possible du système. Pratiquement, toutes les publications sur les turbo-codes font face à des systèmes idéaux où les problèmes de synchronisation ont été résolus parfaitement. Ces hypothèses sont généralement impossibles à satisfaire dans la réalité. Tenir compte de cet aspect est primordial car les turbo-codes s'avèrent être très sensibles aux erreurs de phase et de résidu de fréquence.

– Effet d'un résidu de phase sur la performance des turbo-codes :

Un décalage de phase est inévitable dans les systèmes réels, principalement en raison de l'estimation imparfaite du canal dans des environnements à évanouissement rapide. Le TEB du code avec différents déphasages (supposés constants) $\phi \in [-\frac{\pi}{4}, \frac{\pi}{4}]$ a révélé qu'un turbo-code a une région d'insensibilité relative à une erreur de phase. En dehors de cette région,

cependant, le taux d'erreurs binaire commence à se dégrader rapidement. Une des façons d'améliorer le rendement du turbo code consiste donc à réduire la queue de la distribution de l'erreur de phase. Ceci permet de substituer de larges erreurs qui sont moins probables par de petites erreurs plus fréquentes.

Pour pouvoir évaluer la qualité de l'estimation de cette nouvelle classe d'estimateurs codés, la borne de Cramér-Rao (BCR) est une borne fondamentale dans la théorie de l'estimation, vu qu'elle établit la variance minimale que peut atteindre n'importe quel estimateur non biaisé du paramètre considéré. Cette borne est aussi connue pour être atteignable assymptotiquement, par l'estimateur du maximum de vraisemblance stochastique. Néanmoins, même dans le cas des transmissions non codées, la structure complexe de la fonction de vraisemblance rend la tâche de trouver une expression analytique pour la BCR stochastique très difficile, voire impossible, dans le cas de symboles transmis aléatoirement, surtout dans les modulations d'ordre élevé. Pour celà, elle est généralement évaluée (dans les transmissions codées et non codées) empiriquement[45]. Dans le contexte de l'estimation DA du RSB, l'expression analytique de BCR DA a été dérivée dans [21]. Dans le cas non assisté, les expressions analytiques pour la BCR ont été dérivées aussi, mais pour le cas des modulations BPSK et QPSK. Ce n'était que récemment qu'une expression analytique a été établie dans le cas général des modulations QAM carrées [22, 23]. Dans les

systèmes codés, cependant, la fonction de vraisemblance devient encore plus compliquée. De ce fait, développer une expression analytique de la BCR dans ce cas devient une tâche beaucoup plus laborieuse. À présent, la BCR pour l'estimation du RSB à partir de transmissions codées n'a été établie que dans le cas de la modulation BPSK dans [9].

En ce qui concerne la phase du canal et le résidu de la fréquence porteuse, ces bornes ont été évaluées empiriquement dans le cas PSK et QAM dans [40]. Ce n'était que récemment qu'une expression analytique de la BCR a été établie dans le cas non assisté (NDA) pour la phase du canal et le résidu de fréquence dans [41], avec des signaux QAM carrés. Dans le cas d'une transmission codée, la BCR a été établie par Noels grâce à une approche empirique [42]. Motivés par ces facteurs, nous dérivons dans ce mémoire, pour la première fois[43, 44], une expression analytique pour la BCR de l'estimation du RSB, de la phase du canal et du résidu de la fréquence porteuse pour les modulations BPSK, MSK et QAM carrées. On établira que ces nouvelles bornes analytiques coincident avec les BCRs empiriques qui ont été évaluées précédemment.

Nous montrerons que la BCR codée est inférieure à la BCR non assistée, particulièrement à des moyens et bas RSBs, ce qui reflète l'amélioration considérable qu'apporterait potentiellement la prise en compte du processus de codage dans l'estimation non assistée. Nous remarquerons que

la BCR décroît quand l'ordre de modulation augmente et s'approche de plus en plus de la BCR dans le cas Data Aided, spécialement à bas RSB, contrairement au cas de l'estimation NDA. Nous étudierons en plus l'effet du taux de codage sur la BCR codée et nous établirons que plus le taux de codage est petit (ce qui implique l'ajout de plus de bits de redondance au niveau du codage et donc intuitivement une amélioration de la performance globale du système), plus la BCR est inférieure et s'apprécie de la DA BCR. Cet effet sera plus marqué à bas RSB. À hauts RSB, toutes les bornes convergent.

Chapitre 1

Introduction

Modern wireless communication systems rely on the *a priori* knowledge of the propagation conditions in order to enhance their capacity. In particular, the SNR, the channel phase and the carrier frequency offset(CFO) are considered as key parameters whose *a priori* knowledge can be exploited at both the receiver and the transmitter (through feedback), in order to reach the desired enhanced/optimal performance (using various adaptive schemes). For instance, the SNR level is a key measure of the channel quality [1] and it is, therefore required in multiple applications such as equalization [2, 3], adaptive modulation, link adaptation, and power control [4, 5], just to name a few.

Roughly speaking, SNR, phase and CFO estimators can be broadly divided into two major

categories : i) data-aided (DA) techniques in which the estimation process relies on a perfectly known transmitted sequence, and ii) non-data-aided (NDA) techniques where the estimation process is applied blindly using the received samples only.

Most interestingly, the NDA approaches share the advantage of not impinging on the whole throughput of the system (high spectral efficiency). However, they usually exhibit very poor estimation performance in the low SNR region especially in presence of short data records. To circumvent this problem while being spectrally efficient, code-aided estimation can be envisaged to substantially enhance the performance in these harsh operating conditions. In the same context, turbo codes [6-8] have gained considerable attention during the last two decades thanks to their impressive ability to operate in near-shannon limit even at very low SNR levels.

Very recently, it has been shown that the SNR (in [9-12]) and phase/CFO (in [24,25] and [29-39]) estimation performance can be substantially enhanced by exploiting some priors¹ that are delivered during the decoding process of the transmitted bits. More specifically, it was shown that code-aided (CA) estimation provides — over a wide range of practical SNRs — almost the

1. Note that in the code-aided estimation scheme the transmitted symbols are also completely unknown.

But, much information can be obtained about these symbols during the process of iterative decoding of both the *information* and *redundancy* bits. This knowledge is then used during the estimation process as a *prior* information.

same performance as in the ideal case where all the bits are perfectly *a priori* known (DA). In turbo-coded systems, for instance, CA estimation schemes may rely on the soft information (as priors) obtained from the soft-input soft-output (SISO) decoder. The optimal SISO algorithm [in the sense of minimum bit error rate (BER)] to be used is the maximum a posteriori (MAP), also known as the BCJR algorithm [13, 14]. Yet, the successful implementation of the MAP decoder itself requires the *a priori* knowledge (i.e., estimation) of the SNR [14]. Therefore, the effect of the SNR mismatch on the performance of turbo-decoding has been the subject of various studies [16-18]. It was found, in the particular case of BPSK signals, that over-estimating the SNR by several dBs can be tolerated while insuring acceptable BER performance. In contrast, under-estimation by more than 2 dB leads to significant decoding errors. In presence of higher-order-modulated signals, the effect of SNR mismatch was also investigated in [20] and found to be remarkably different from its counterpart in BPSK signalling. The estimated SNR plays a different role in the calculation of the bit metrics for various modulation schemes, and therefore leads to different decoding performances. The performance of turbo-coded systems, transmitting higher-order-modulated signals, is typically more sensitive to over-estimating the SNR [20].

In the case of the phase and CFO, the impressive performance of turbo codes can be achieved

in conjunction with a coherent detection scheme only. This means that the carrier phase and carrier frequency offset (CFO) must be accurately acquired before proceeding to data decoding. This is because turbo codes are known to be very sensitive to phase errors and even a small mismatch in the carrier phase can lead to severe performance degradations. In fact, it has been seen that the turbo code has a *region* of a relative sensitivity to phase error, outside of which, the bit error rate (BER) starts to deteriorate quickly.

Accurate synchronization has always been challenging in turbo-coded systems, since they are intended to operate at low signal-to-noise ratios (SNRs). Many SNR, phase and CFO estimators suited for turbo-coded systems have been recently introduced in the open literature [9-12] and [24,25,29-39]. The performance of such code aided SNR, CFO and phase estimators is usually assessed in terms of their variances for which an absolute benchmark must be evaluated. The Cramér-Rao lower bound (CRLB), a well known fundamental bound [27] in estimation theory, meets this requirement since it sets the minimum achievable variance for all the unbiased estimators. Unlike other loose bounds, the CRLB is also known to be achieved, asymptotically, by the stochastic maximum likelihood estimator. Yet, even in case of uncoded transmissions, the complex structure of the likelihood function makes it extremely hard, if not impossible, to derive analytical expressions for the *stochastic*² CRLB, especially for higher-order modulations.

2. The stochastic designation is usually adopted to refer to the case of unknown and random transmitted

Therefore, it is usually evaluated (in both non-coded and coded systems) empirically[45].

Within the context of DA SNR estimation, the closed-form expressions for the DA CRLBs were earlier derived in [21]. The analytical expressions for the exact NDA CRLBs were also derived in the same work but only in the very special cases of BPSK and QPSK signals. It was only recently that these analytical expressions have been generalized to arbitrary higher-order square QAM modulations [22, 23]. In coded transmissions, however, the likelihood function becomes even more complicated and hence developing the corresponding bounds in closed-form expressions is a more challenging task. Thus, code-aided SNR estimators are usually compared in performance to the DA CRLBs as has been recently done in [12, 15]. The latter may be an accurate benchmark for BPSK signals but is actually an excessively optimistic³ bound in presence of higher-order-modulated signals, especially at low SNR values. To date, the CRLB for code-aware SNR estimation has been recently tackled in [9] but only for the very basic case of BPSK-modulated signals. In the case of the phase and CFO estimation, the CRLBs for these estimation were evaluated empirically for the uncoded PSK- and symmetric-QAM-modulated signals in [40]. It was only recently that closed-form expressions for the stochastic CRLBs have

symbols. This is to be opposed to the *deterministic* CRLB when the symbols are unknown but deterministic.

3. The DA CRLBs are indeed the same for all the linearly-modulated signals [21], i.e., they wrongly reflect the same benchmark irrespectively of the modulation type or order.

been established in [41] for NDA carrier phase and CFO estimation, from general square QAM-modulated signals. In coded transmissions, however, the likelihood function becomes even more complicated and developing such bounds in closed form is therefore more challenging and tedious. Thus, the CRLB for phase and CFO estimation of coded linearly-modulated signals was earlier tackled by Noels *et al.* in [42] through an empirical approach. Motivated by these facts, we derive in this work, for the first time, the analytical expressions for the CRLBs of SNR, channel phase and CFO estimates from coded BPSK-, MSK- and arbitrary square-QAM-modulated signals. It will be seen that the new analytical CRLBs coincide with their empirical counterparts derived in this report as well for a matter of validation.

The rest of this report is organized as follows. In chapter II, we introduce the system model. In chapter III, we derive the explicit expression for the loglikelihood function for the different transmissions. In chapter IV, we derive new analytical expressions for the corresponding CRLBs and we propose, as well, another approach that allows the evaluation of the considered bounds empirically. In chapter V, we present the simulation results of the newly derived bounds. Finally, we draw out some concluding remarks in chapter VI.

We also mention that some of the common notations will be used throughout this paper. Indeed, vectors and matrices are represented in lower- and upper-case bold fonts, respectively.

Moreover, $\{.\}^T$ and $\{.\}^H$ denote the transpose and the Hermitian (transpose conjugate) operators, respectively. The operators $\Re\{.\}$ and $\Im\{.\}$, $|.|$ return, respectively, the real, imaginary parts and the amplitude of any complex number whereas $\{.\}^*$ returns its conjugate. We also denote by j the pure complex number that verifies $j^2 = -1$. We will also denote the probability mass function (PMF) for discrete random variables by $P[.]$ and the probability density function (pdf) for continuous random variables by $p(.)$.

Chapitre 2

System Model

Consider a turbo-coded system where a binary sequence of information bits (grouped into consecutive blocks containing Q bits each) is fed into a turbo encoder, of rate R , consisting of two identical recursive systematic convolutional codes (RSCs) with generator polynomials $[g1, g2]$. The two RSCs are concatenated in parallel via an interleaver of size L . The coded bits are then fed into a puncturer which selects an appropriate combination of the parity bits, from both encoders, in order to achieve the desired overall rate R . Each block of Q coded bits (systematic and parity bits) is then interleaved with an outer interleaver, and then mapped onto any Gray-coded constellation¹. Finally, the obtained symbols are transmitted over the wireless channel. The received signal is sampled at the output of the matched filter. Then by

1. We shall later restrict ourselves to BPSK, MSK and square-QAM constellations only.

assuming *imperfect* phase and frequency synchronization, the observed samples are modeled as follows :

$$\begin{aligned} y(k) &= S x(k) e^{j2\pi k\vartheta + \phi} + w(k), \\ k &= k_0, 1, 2, \dots, k_0 + K - 1, \end{aligned} \tag{2.1}$$

where, at time index k , $x(k)$ is the transmitted coded symbol and $y(k)$ is the corresponding received sample. The noise components are modeled by a zero-mean circular complex Gaussian random variable, with independent real and imaginary parts, each of variance σ^2 (i.e., a total noise power, N_0 , of $N_0 = 2\sigma^2$). The parameters S and K stand for the channel gain and the total number of received samples, respectively. Without loss of generality, we further assume that the energy of the transmitted symbols is normalized² to one, i.e., $E\{|x(k)|^2\} = 1$. Using the multiple observations $\{y(k)\}_{k=k_0}^{k_0+K-1}$, the true SNR, ρ , that we wish to estimate, is defined as

$$\rho = \frac{E\{S^2|x(k)|^2\}}{2\sigma^2}, \tag{2.2}$$

$$= \frac{S^2}{2\sigma^2}. \tag{2.3}$$

2. If the transmit energy, P , is not unitary, then it can be easily incorporated as an unknown scaling factor into the channel coefficients by estimating $\tilde{S} = \sqrt{P}S$ instead of S in (2.1).

From (2.3), it is seen that there are two unknown parameters which are involved in the derivation of the SNR CRLBs, which are : S and σ^2 . Therefore, it is mathematically more convenient to gather them in one signle parameter vector :

$$\boldsymbol{\alpha}^{(1)} = [S \quad \sigma^2]. \quad (2.4)$$

In addition, since using the decibel (dB) scale often provides easier interpretation of the performance behaviour, we will henceforth consider the following parameter transformation :

$$g(\boldsymbol{\alpha}^{(1)}) = 10 \log_{10} \left(\frac{S^2}{2\sigma^2} \right). \quad (2.5)$$

For mathematical convenience, we gather all the recorded data samples in a single vector :

$$\mathbf{y} = [y(0), y(1), \dots, y(K-1)]^T. \quad (2.6)$$

Notice that we used the index $k = 0, 1, \dots, K-1$ instead of $k = k_0, \dots, k_0 + K - 1$, when considering the particular case of SNR estimation (represented by $\alpha^{(1)}$, since it has no effect on the CRLB of the SNR, even intuitively. The log-likelihood function of the system will be denoted as

$L_{\mathbf{y}}(\boldsymbol{\alpha}^{(1)}) = \ln(p(\mathbf{y}; \boldsymbol{\alpha}^{(1)}))$ where $p(\mathbf{y}; \boldsymbol{\alpha}^{(1)})$ is the pdf of the received vector \mathbf{y} parameterized by the unknown parameter vector $\boldsymbol{\alpha}^{(1)}$. As shown in [27], the CRLB for parameter transformations is given by

$$\text{CRLB}(\rho) = \frac{\partial g(\boldsymbol{\alpha}^{(1)})}{\partial \boldsymbol{\alpha}^{(1)}} \mathbf{I}^{-1}(\boldsymbol{\alpha}^{(1)}) \frac{\partial g(\boldsymbol{\alpha}^{(1)})}{\partial \boldsymbol{\alpha}^{(1)}}^T, \quad (2.7)$$

where the derivative of the parameter transformation, $\partial g(\boldsymbol{\alpha}^{(1)})/\partial \boldsymbol{\alpha}^{(1)}$, is given by

$$\frac{\partial g(\boldsymbol{\alpha}^{(1)})}{\partial \boldsymbol{\alpha}^{(1)}} = \begin{bmatrix} 20 & -10 \\ \ln(10)S & \ln(10)\sigma^2 \end{bmatrix}, \quad (2.8)$$

and $\mathbf{I}(\boldsymbol{\alpha}^{(1)})$ is the Fisher information matrix (FIM) defined as :

$$\mathbf{I}(\boldsymbol{\alpha}^{(1)}) = \begin{pmatrix} -E\left\{\frac{\partial^2 L_{\mathbf{y}}(\boldsymbol{\alpha}^{(1)})}{\partial S^2}\right\} - E\left\{\frac{\partial^2 L_{\mathbf{y}}(\boldsymbol{\alpha}^{(1)})}{\partial S \partial \sigma^2}\right\} \\ -E\left\{\frac{\partial^2 L_{\mathbf{y}}(\boldsymbol{\alpha}^{(1)})}{\partial \sigma^2 \partial S}\right\} - E\left\{\frac{\partial^2 L_{\mathbf{y}}(\boldsymbol{\alpha}^{(1)})}{\partial \sigma^2}\right\} \end{pmatrix}. \quad (2.9)$$

In (2.9), the statistical expectation $E\{\cdot\}$ is taken with respect to \mathbf{y} . Usually, the analytical derivation of the CRLB involves tedious algebraic manipulations. These consist in three major steps : 1) derivation of the log-likelihood function (LLF), 2) derivation of the FIM elements and then 3) derivation of the CRLB expression using (2.7). These three steps will be accomplished, in this order, in the remainder of this report.

The parameters ϕ and ϑ stand for the phase distortion and the carrier frequency offset, both to be estimated (separately from the channel gain S and the noise variance σ^2 , respectively).

Both unknown parameters are gathered into one vector

$$\boldsymbol{\alpha}^{(2)} = [\phi \quad \vartheta]^T. \quad (2.10)$$

and the received samples into one vector :

$$\mathbf{y} = [y(k_0), y(k_0 + 1), \dots, y(k_0 + K - 1)]^T. \quad (2.11)$$

Now, suppose that we are able to produce an unbiased estimate, $\hat{\boldsymbol{\alpha}}^{(2)}$, of the vector $\boldsymbol{\alpha}^{(2)}$, from the received vector \mathbf{y} . Then the CRLB, verifying³ the inequality $E \{ [\hat{\boldsymbol{\alpha}}^{(2)} - \boldsymbol{\alpha}^{(2)}]^T [\hat{\boldsymbol{\alpha}}^{(2)} - \boldsymbol{\alpha}^{(2)}] \} \succeq \mathbf{CRLB}(\boldsymbol{\alpha}^{(2)})$, is given by :

$$\mathbf{CRLB}(\boldsymbol{\alpha}^{(2)}) = \mathbf{I}^{-1}(\boldsymbol{\alpha}^{(2)}), \quad (2.12)$$

where $\mathbf{I}(\boldsymbol{\alpha}^{(2)})$ is the Fisher information matrix (FIM) whose entries are given by :

$$[\mathbf{I}(\boldsymbol{\alpha}^{(2)})]_{i,l} = -E_{\mathbf{y}} \left\{ \frac{\partial^2 L_{\mathbf{y}}(\boldsymbol{\alpha}^{(2)})}{\partial \alpha_i^{(2)} \partial \alpha_l^{(2)}} \right\} \quad i, l = 1, 2 \quad (2.13)$$

where $\left\{ \alpha_i^{(2)} \right\}_{i=1,2}$ are the elements of the vector $\boldsymbol{\alpha}^{(2)}$.

3. Note that $\mathbf{A} \succeq \mathbf{B}$ for any two \mathbf{A} and \mathbf{B} square matrices means that $\mathbf{A} - \mathbf{B}$ is positive semi-definite.

Chapitre 3

Derivation of the Log-Likelihood Function (LLF)

To begin with, we assume that the symbols are drawn from any $M - ary$ constellation whose alphabet is denoted as $\mathcal{C} = \{c_0, c_1, \dots, c_M\}$. This is because, as will be seen shortly, the first derivation steps are valid for linearly-modulated signals in general. However, we will later on restrict ourselves to BPSK, MSK or square-QAM constellations and the reasons will be clearly stated. In the sequel, the constellation is assumed to be Gray-coded and we use the following

two notations :

$$c_m \longleftrightarrow \bar{b}_1^m \bar{b}_2^m \cdots \bar{b}_l^m \cdots \bar{b}_{\log_2(M)}^m \quad (3.1)$$

$$x(k) \longleftrightarrow b_1^k b_2^k \cdots b_l^k \cdots b_{\log_2(M)}^k. \quad (3.2)$$

to designate the mapping between the m^{th} constellation point c_m (respectively, the k^{th} transmitted symbol $x(k)$) and its associated bits (respectively, the k^{th} conveyed bits). Due to the large-size interleaver, the coded bits can be assumed independent. Such an assumption is pervasive in code-aided estimation [10, 24, 25, 28]. Consequently, the transmitted symbols (which originate simply from a mapping of these independent bits) can also be considered as independent yielding thereby :

$$p(\mathbf{y}; \boldsymbol{\alpha}) = \prod_{k=k_0}^{k_0+K-1} p(y(k); \boldsymbol{\alpha}), \quad (3.3)$$

where $p(y(k); \boldsymbol{\alpha})$ is the pdf of the individual received sample, $y(k)$, which is given by :

$$\begin{aligned} p(y(k); \boldsymbol{\alpha}) &= \sum_{c \in \mathcal{C}} P[x(k) = c] p(y(k); \boldsymbol{\alpha} | x(k) = c), \\ &= \sum_{m=0}^M \frac{P[x(k) = c_m]}{2\pi\sigma^2} \exp\left\{-\frac{|y(k) - S_{\phi,\vartheta} c_m|^2}{2\sigma^2}\right\}. \end{aligned} \quad (3.4)$$

where

$$S_{\phi,\vartheta} = S e^{j2\pi k\vartheta + \phi}. \quad (3.5)$$

and

$$\boldsymbol{\alpha} = [\boldsymbol{\alpha}^{(1)} \quad \boldsymbol{\alpha}^{(2)}]. \quad (3.6)$$

Now, in case of higher-order modulations where each constellation point represents more than one bit (i.e., $M > 2$ or equivalently $\log_2(M) > 1$) and again due to the independence of the coded bits, the probability of each transmitted symbol, $x(k)$, factors into the elementary probabilities of the elementary bits it conveys :

$$\begin{aligned} P[x(k) = c_m] &= P\left[b_1^k = \bar{b}_1^m, \dots, b_{\log_2(M)}^k = \bar{b}_{\log_2(M)}^m\right] \\ &= \prod_{l=1}^{\log_2(M)} P\left[b_l^k = \bar{b}_l^m\right]. \end{aligned} \quad (3.7)$$

We also define the so-called log-likelihood ratio (LLR) of the coded transmitted bit b_l^k as follows :

$$L_l(k) = \ln \left(\frac{Pr[b_l^k = 1]}{Pr[b_l^k = 0]} \right). \quad (3.8)$$

Then, using (3.8) and the fact that $P[b_l^k = 0] + P[b_l^k = 1] = 1$, the *a priori* probabilities of the coded transmitted bits can be expressed as :

$$P[b_l^k = 1] = \frac{e^{L_l(k)}}{1 + e^{L_l(k)}} = \frac{1}{2} \operatorname{sech} \left(\frac{L_l(k)}{2} \right) e^{\frac{L_l(k)}{2}}, \quad (3.9)$$

and

$$P[b_l^k = 0] = \frac{1}{1 + e^{L_l(k)}} = \frac{1}{2} \operatorname{sech} \left(\frac{L_l(k)}{2} \right) e^{-\frac{L_l(k)}{2}}. \quad (3.10)$$

3.1 LLF for BPSK and MSK signals :

In BPSK transmissions, the constellation alphabet is given by $\mathcal{C} = \{+1, -1\}$. In MSK transmissions, however, the transmitted symbols are constructed recursively as $x(k+1) = jx(k)(2b_k - 1)$ where b_k is the sequence of coded bits and $x(k_0)$ is the original value drawn from the set $\{-1, -j, +1, +j\}$. The pdf of the received vector \mathbf{y} parameterized by $\boldsymbol{\alpha}$ is expressed as follows :

$$p(\mathbf{y}; \boldsymbol{\alpha}) = \prod_{k=k_0}^{k_0+K-1} \left(\frac{P[x(k) = d_k]}{2\pi\sigma^2} \exp \left\{ -\frac{|y(k) - d_k S_{\phi,\vartheta}|^2}{2\sigma^2} \right\} \right. \\ \left. + \frac{P[x(k) = -d_k]}{2\pi\sigma^2} \exp \left\{ -\frac{|y(k) + d_k S_{\phi,\vartheta}|^2}{2\sigma^2} \right\} \right). \quad (3.11)$$

in which d_k is given by :

$$d_k = \begin{cases} 1 & \text{for BPSK} \\ j^{k-1} k(k_0) & \text{for MSK.} \end{cases} \quad (3.12)$$

Then, we define the log-likelihood ratio (LLR) of the coded bits :

$$L(k) = \ln \left(\frac{P[b_k = 1]}{P[b_k = 0]} \right). \quad (3.13)$$

Note here that, for the sake of clarity, we use two different designations for the constellation points, d_k , in (3.12) and the actual transmitted bits, b_k , in (3.13). Yet, statistically speaking, they both have the same probabilities. That is to say : $P[d_k = 1] = P[b_k = 1]$, $P[d_k = -1] = P[b_k = 0]$ in BPSK and $P[d_k = j^{k-1}x(k_0)] = P[b_k = 1]$, $P[d_k = -j^{k-1}x(k_0)] = P[b_k = -1]$ in

MSK. Injecting these results in (3.11) and after some algebraic manipulations, it can be shown that the log-likelihood function of interest (after dropping terms independent of the parameters gathered in $\boldsymbol{\alpha}$) denoted by $L_{\mathbf{y}}^{(r)}(\boldsymbol{\alpha})$ is expressed as follows :

$$\begin{aligned} L_{\mathbf{y}}^{(r)}(\boldsymbol{\alpha}) = & -K \ln(\sigma^2) - \frac{KS^2}{2\sigma^2} - \frac{1}{2\sigma^2} \sum_{k=k_0}^{k_0+K-1} |y(k)|^2 \\ & + \sum_{k=k_0}^{k_0+K-1} \ln \left(\cosh \left(\frac{\Re(y(k)^* d_k S_{\phi,\vartheta})}{\sigma^2} + \frac{L(k)}{2} \right) \right). \end{aligned} \quad (3.14)$$

3.2 LLF for QPSK signals :

We denote the constellation alphabet, \mathcal{C} , of the QPSK constellation as $\mathcal{C} = \{c_0, c_1, c_2, c_3\}$.

Therefore, the pdf of the received sample, $y(k)$, is given by :

$$\begin{aligned} p(y(k); \boldsymbol{\alpha}) = & \sum_{c \in \mathcal{C}} P[x(k) = c] p(y(k); \boldsymbol{\alpha} | x(k) = c), \\ = & \sum_{m=0}^3 \frac{P[x(k) = c_m]}{2\pi\sigma^2} \exp \left\{ \frac{|y(k) - S_{\phi,\vartheta} c_m|^2}{2\sigma^2} \right\}. \end{aligned} \quad (3.15)$$

Without loss of generality, we assume that $c_0 = 1/\sqrt{2} + j/\sqrt{2}$ and that the constellation is Gray coded according to the following mapping : $c_0 \longleftrightarrow 11$, $c_1 \longleftrightarrow 10$, $c_2 \longleftrightarrow 00$ and

$c_3 \longleftrightarrow 01$. Consequently, from (3.10) and (3.9), we obtain :

$$P[x(k) = c_0] = \frac{e^{L_1(k)}}{1 + e^{L_1(k)}} \frac{e^{L_2(k)}}{1 + e^{L_2(k)}}, \quad (3.16)$$

$$P[x(k) = c_1] = \frac{e^{L_1(k)}}{1 + e^{L_1(k)}} \frac{1}{1 + e^{L_2(k)}}, \quad (3.17)$$

$$P[x(k) = c_2] = \frac{1}{1 + e^{L_1(k)}} \frac{1}{1 + e^{L_2(k)}}, \quad (3.18)$$

$$P[x(k) = c_3] = \frac{1}{1 + e^{L_1(k)}} \frac{e^{L_2(k)}}{1 + e^{L_2(k)}}. \quad (3.19)$$

Then, by using the fact that $c_1 = -c_0$, $c_2 = c_0^*$ and $c_3 = -c_0^*$, plugging (3.16) to (3.19) back into (3.15), and after some algebraic manipulations, it can be shown that :

$$\begin{aligned} p(y(k); \boldsymbol{\alpha}) &= \frac{1}{2\pi\sigma^2} \exp\left\{-\frac{S^2 + |y(k)|^2}{2\sigma^2}\right\} \\ &\times Q_1(k) \cosh\left(\frac{\Re\{y(k)^* S_{\phi,\vartheta}\}}{\sigma^2} + \frac{L_2(k)}{2}\right) \\ &\times Q_2(k) \cosh\left(\frac{\Im\{y(k)^* S_{\phi,\vartheta}\}}{\sigma^2} - \frac{L_1(k)}{2}\right), \end{aligned} \quad (3.20)$$

where

$$Q_l(k) = \frac{1}{\cosh(L_l(k)/2)} \quad (3.21)$$

Thus, the pdf of the received vector \mathbf{y} is factorized as follows :

$$\begin{aligned} p(\mathbf{y}; \boldsymbol{\alpha}) &= C_{\mathbf{y}}(\boldsymbol{\alpha}) \prod_{k=k_0}^{k_0+K-1} Q_1(k) \cosh\left(\frac{\Re(y(k)^* S_{\phi,\vartheta})}{\sigma^2} + \frac{L_2(k)}{2}\right) \\ &\times \prod_{k=k_0}^{k_0+K-1} Q_2(k) \cosh\left(\frac{\Im(y(k)^* S_{\phi,\vartheta})}{\sigma^2} - \frac{L_1(k)}{2}\right), \end{aligned} \quad (3.22)$$

where

$$C_y(\boldsymbol{\alpha}) = \frac{1}{\sigma^{2K}(2\pi)^K} \exp \left\{ -\frac{KS^2}{2\sigma^2} - \frac{1}{2\sigma^2} \sum_{k=k_0}^{k_0+K-1} |y(k)|^2 \right\}. \quad (3.23)$$

By, taking the logarithm of (3.22) and dropping the constant terms involving $Q_1(k)$ and $Q_2(k)$ (which do not depend on $\boldsymbol{\alpha}$), the LLF for QPSK signals develops as follows :

$$\begin{aligned} L_y^{(r)}(\boldsymbol{\alpha}) = & -K \ln(\sigma^2) - \frac{KS^2}{2\sigma^2} - \frac{1}{2\sigma^2} \sum_{k=k_0}^{k_0+K-1} |y(k)|^2 + \\ & \sum_{k=k_0}^{k_0+K-1} \ln \left(\cosh \left(\frac{\Re \{y(k)^* d_k S_{\phi,\vartheta}\}}{\sigma^2} + \frac{L_2(k)}{2} \right) \right) + \\ & \sum_{k=k_0}^{k_0+K-1} \ln \left(\cosh \left(\frac{\Im \{y(k)^* d_k S_{\phi,\vartheta}\}}{\sigma^2} + \frac{L_1(k)}{2} \right) \right). \end{aligned} \quad (3.24)$$

3.3 LLF for square-QAM signals :

Denoting $I(k) = \Re\{y(k)\}$ and $Q(k) = \Im\{y(k)\}$, it can be shown that in presence of M -ary QAM-modulated signals, the pdf in (3.4) can be rewritten as follows :

$$p(y(k); \boldsymbol{\alpha}) = \frac{1}{2\pi\sigma^2} \exp \left\{ -\frac{I(k)^2 + Q(k)^2}{2\sigma^2} \right\} D_{\boldsymbol{\alpha}}(k), \quad (3.25)$$

in which

$$\begin{aligned} D_{\boldsymbol{\alpha}}(k) = & \sum_{m=1}^M P_m[x_k] \exp \left\{ -\frac{S^2 |c_m|^2}{2\sigma^2} \right\} \times \\ & \exp \left\{ \frac{\Re \{c_m y(k)^* S_{\phi,\vartheta}\}}{\sigma^2} \right\}, \end{aligned} \quad (3.26)$$

where

$$P_m[x_k] = \Pr\{x_k = c_m\}. \quad (3.27)$$

Hence, the LLF ($L_{\mathbf{y}}(\alpha) = \ln \{p(\mathbf{y}; \boldsymbol{\alpha})\}$) which is obtained from (3.3) as $L_{\mathbf{y}}(\alpha) = \sum_{k=k_0}^{k_0+K-1} \ln\{p(y(k); \boldsymbol{\alpha})\}$,

develops into :

$$\begin{aligned} L_{\mathbf{y}}(\boldsymbol{\alpha}) = & -K \ln \{2\pi\sigma^2\} - \sum_{k=k_0}^{k_0+K-1} \frac{I(k)^2 + Q(k)^2}{2\sigma^2} \\ & + \sum_{k=k_0}^{k_0+K-1} \ln\{D_{\boldsymbol{\alpha}}(k)\}. \end{aligned} \quad (3.28)$$

At this stage, it is still very tedious to derive analytical expressions for the considered CRLBs without further developing the terms $D_{\boldsymbol{\alpha}}(k)$ defined in (3.26). Actually, considering the special case of square QAM-modulated signals (i.e., 4-, 16-, 64-QAM, etc.), and by exploring the structure of the Gray mapping mechanism, we are able to factor $D_{\boldsymbol{\alpha}}(k)$ into the product of two analogous terms. In fact, when $M = 2^{2p}$ for any $p \geq 1$ (i.e., square QAM constellations), we have

$\mathcal{C} = \{\pm(2i-1)d_p \pm j(2n-1)d_p\}_{i,n=1,2,\dots,2^{p-1}}$, where $2d_p$ is the intersymbol distance in the I/Q

plane. The square QAM constellation energy is supposed to be normalized to one :

$$\frac{\sum_{m=1}^{2^{2p}} |c_m|^2}{2^{2p}} = 1, \quad (3.29)$$

from which the expression of d_p is obtained as follows :

$$d_p = \frac{2^{p-1}}{\sqrt{2^p \sum_{m=1}^{2^{p-1}} (2m-1)^2}}. \quad (3.30)$$

Now, by denoting $\tilde{\mathcal{C}} = \{(2i-1)d_p + j(2n-1)d_p\}_{i,n=1}^{2^{p-1}}$ the subset of the alphabet that consists of the points which lie in the top-right quadrant of the constellation, one can write $\mathcal{C} = \tilde{\mathcal{C}} \cup (-\tilde{\mathcal{C}}) \cup \tilde{\mathcal{C}}^* \cup (-\tilde{\mathcal{C}}^*)$. Therefore (3.26) can be expressed as follows :

$$\begin{aligned} D_{\alpha}(k) = & \sum_{\tilde{c}_m \in \tilde{\mathcal{C}}} \exp \left\{ -\frac{S^2 |\tilde{c}_m|^2}{2\sigma^2} \right\} \times \\ & \left(P[x_k = \tilde{c}_m] \exp \left\{ \frac{\Re \{ \tilde{c}_m y^*(k) S_{\phi,\vartheta} \}}{\sigma^2} \right\} \right. \\ & + P[x_k = -\tilde{c}_m] \exp \left\{ \frac{\Re \{ -\tilde{c}_m y^*(k) S_{\phi,\vartheta} \}}{\sigma^2} \right\} \\ & + P[x_k = \tilde{c}_m^*] \exp \left\{ \frac{\Re \{ \tilde{c}_m^* y^*(k) S_{\phi,\vartheta} \}}{\sigma^2} \right\} \\ & \left. + P[x_k = -\tilde{c}_m^*] \exp \left\{ \frac{\Re \{ -\tilde{c}_m^* y^*(k) S_{\phi,\vartheta} \}}{\sigma^2} \right\} \right). \end{aligned} \quad (3.31)$$

Another important detail that must be addressed, in order to further simplify the term $D_{\alpha}(k)$, is the Gray mapping scheme of the constellation. We will show through a simple Gray-coding mechanism how this structure can be used to factor $D_{\alpha}(k)$, linearizing thereby the LLF expression in (3.28). The procedure applies in the same way to all the possible Gray mapping schemes, and the obtained final CRLB expressions are the same. First, combining (3.9) and (3.10) and assuming that the symbol c_m is transmitted during the k^{th} time instant (i.e., $x(k) = c_m$), we obtain the following generic formula for each conveyed bit :

$$P[b_l^k = \bar{b}_l^m] = \frac{1}{2} \operatorname{sech} \left(\frac{L_l(k)}{2} \right) e^{(2\bar{b}_l^m - 1) \frac{L_l(k)}{2}}, \quad (3.32)$$

where \bar{b}_l^m can be 0 or 1. Therefore, recalling that $\log_2(M) = 2p$ and injecting (3.32) in (3.7), the symbol probabilities $P[x_k = c_m]$ are given by :

$$P[x(k) = c_m] = \underbrace{\left(\prod_{l=1}^{2p} \frac{1}{2} \operatorname{sech} \left(\frac{L_l(k)}{2} \right) \right)}_{\beta_k} \times \underbrace{\left(\prod_{l=1}^{2p} e^{(2\bar{b}_l^m - 1) \frac{L_l(k)}{2}} \right)}_{\xi_k(c_m)}. \quad (3.33)$$

Next, we describe a simple recursive algorithm that allows the construction of Gray-coded square-QAM constellations. Some interesting properties of such constellations will be revealed and carefully handled in order to factor the term $D_\alpha(k)$ in (3.31). In fact, starting from any given $2^{2(p-1)}$ -QAM Gray-coded constellation, it is possible to build a 2^{2p} -QAM Gray-coded constellation as follows :

- *step 1* : build the top right quadrant of the desired 2^{2p} -QAM constellation from all the points¹ of the available $2^{2(p-1)}$ -QAM constellation.
- *step 2* : build the other three quadrants of the new 2^{2p} -QAM constellation by symmetries on : i) the x -axis (to obtain the bottom right quadrant), ii) on the y -axis (to obtain the top left quadrant), iii) the center point (to obtain the bottom left quadrant). Yet, the points of the original $2^{2(p-1)}$ -QAM constellation represent $2(p - 1)$ bits only. Therefore, each point of

1. The same points' layout in the original $2^{2(p-1)}$ -QAM constellation is used, i.e., the constellation is placed as is in the new quadrant.

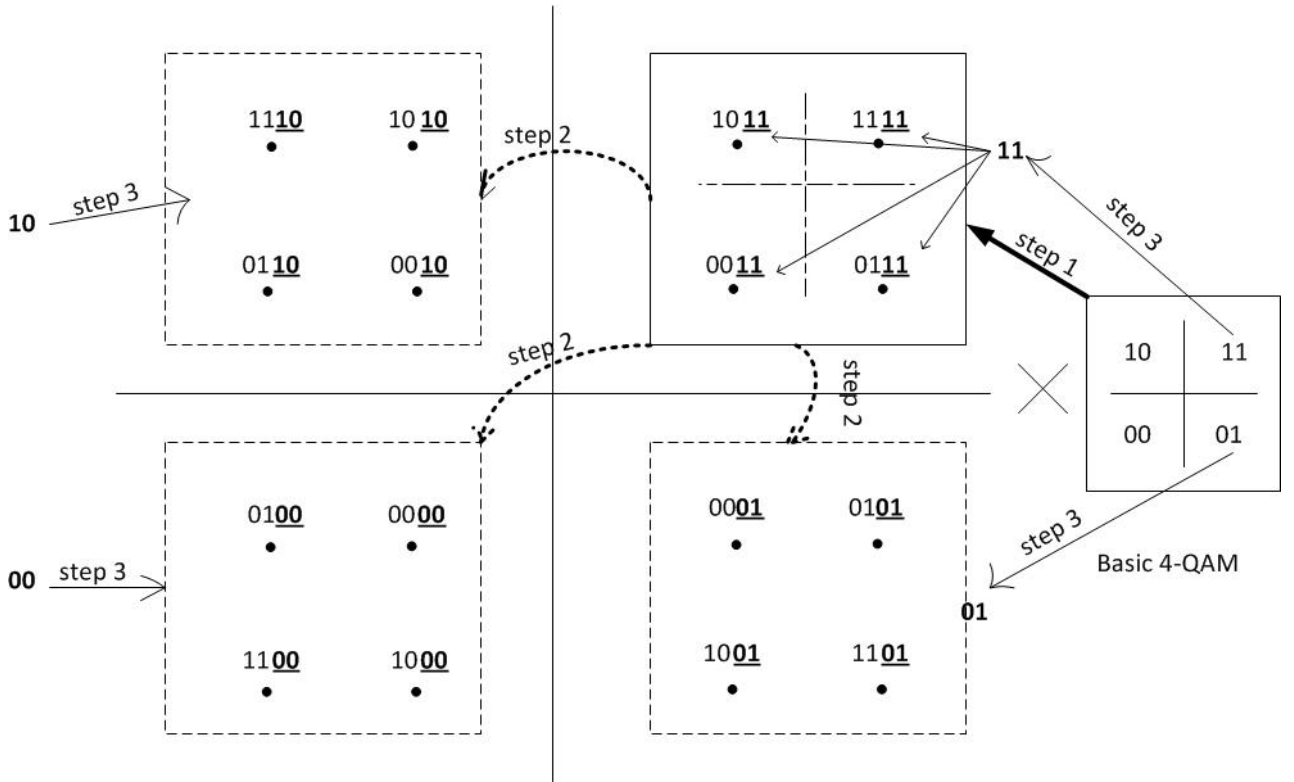


FIGURE 3.1 – Construction of Gray-coded Square-QAM constellations

the new 2^{2p} -QAM constellation that must represent $2p$ bits is still missing two of them.

- *step 3* : add the two bits that appear in each quadrant of a basic Gray-coded QPSK constellation to all the points that appear in the same quadrant of the new constellation.

An example of constructing a Gray-coded 16-QAM constellation from a 4-QAM Gray-coded one is illustrated in Fig. 3.1 Just as depicted in this figure and without loss of generality, we will assume in the sequel that it is the two least significant bits (LSBs) that are always added in “*step 3*”.

Then, due to symmetries in “*step 2*”, it can be seen that each set of four symbols \tilde{c}_m , \tilde{c}_m^* , $-\tilde{c}_m$ and $-\tilde{c}_m^*$ have the same $2(p-1)$ most significant bits (MSBs), $\bar{b}_1^m \bar{b}_2^m \bar{b}_3^m \dots \bar{b}_{2p-3}^m \bar{b}_{2p-2}^m$, for any given symbol \tilde{c}_m from the top right quadrant of the 2^{2p} -QAM constellation ($m = 1, 2, \dots, 2^{2(p-1)}$).

Thus, if we consider these $2(p-1)$ MSBs alone and we define

$$\mu_k(c_m) \triangleq \prod_{l=1}^{2p-2} e^{(2\bar{b}_l^m - 1)\frac{L_l(k)}{2}}, \quad \forall c_m \in \mathcal{C}, \quad (3.34)$$

it can be immediately seen that :

$$\mu_k(\tilde{c}_m) = \mu_k(-\tilde{c}_m) = \mu_k(\tilde{c}_m^*) = \mu_k(-\tilde{c}_m^*), \quad \forall \tilde{c}_m \in \tilde{\mathcal{C}}. \quad (3.35)$$

Now, considering the two remaining LSBs (\bar{b}_{2p-1}^m and \bar{b}_{2p}^m) and using the Gray-mapping depicted in Fig. 3.1, it is seen that for any $\tilde{c}_m \in \tilde{\mathcal{C}}$ we have $\bar{b}_{2p-1}^m \bar{b}_{2p}^m = 11$. Moreover, these two bits are respectively given by “00”, “01”, and “10” for $-\tilde{\mathcal{C}}$, $\tilde{\mathcal{C}}^*$, and $-\tilde{\mathcal{C}}^*$. Of course, these intermediate results change according to the choice of the basic QPSK constellation involved in *step 3*. Yet, we will explain later how this choice does not affect the final result. Then, upon using these

results along with (3.35), it follows from (3.33) that for any $\tilde{c}_m \in \tilde{\mathcal{C}}$, we have :

$$P[x(k)=\tilde{c}_m] = \beta_k \mu_k(\tilde{c}_m) e^{\frac{L_{2p-1}(k)}{2}} e^{\frac{L_{2p}(k)}{2}}, \quad (3.36)$$

$$P[x(k)=\tilde{c}_m^*] = \beta_k \mu_k(\tilde{c}_m) e^{-\frac{L_{2p-1}(k)}{2}} e^{\frac{L_{2p}(k)}{2}}, \quad (3.37)$$

$$P[x(k)=-\tilde{c}_m] = \beta_k \mu_k(\tilde{c}_m) e^{-\frac{L_{2p-1}(k)}{2}} e^{-\frac{L_{2p}(k)}{2}}, \quad (3.38)$$

$$P[x(k)=-\tilde{c}_m^*] = \beta_k \mu_k(\tilde{c}_m) e^{\frac{L_{2p-1}(k)}{2}} e^{-\frac{L_{2p}(k)}{2}}. \quad (3.39)$$

Therefore, plugging these probabilities back into (3.31) and using the identity $e^x + e^{-x} = 2 \cosh(x)$, it can be shown that :

$$\begin{aligned} D_\alpha(k) &= 2\beta_k \sum_{\tilde{c}_m \in \tilde{\mathcal{C}}} \exp \left\{ -\frac{S^2 |\tilde{c}_m|^2}{2\sigma^2} \right\} \mu_k(\tilde{c}_m) \times \\ &\quad \left[\cosh \left(\frac{\Re \{ \tilde{c}_m y^*(k) S_{\phi,\vartheta} \}}{\sigma^2} + \frac{L_{2p-1}(k)}{2} + \frac{L_{2p}(k)}{2} \right) \right. \\ &\quad \left. + \cosh \left(\frac{\Re \{ \tilde{c}_m^* y^*(k) S_{\phi,\vartheta} \}}{\sigma^2} + \frac{L_{2p-1}(k)}{2} - \frac{L_{2p}(k)}{2} \right) \right]. \end{aligned} \quad (3.40)$$

Furthermore, using the relationship $\cosh(x) + \cosh(y) = 2 \cosh(\frac{x+y}{2}) \cosh(\frac{x-y}{2})$ along with the two identities $\tilde{c}_m + \tilde{c}_m^* = 2\Re\{\tilde{c}_m\}$ and $\tilde{c}_m - \tilde{c}_m^* = 2j\Im\{\tilde{c}_m\}$, (3.40) is rewritten as follows :

$$\begin{aligned} D_\alpha(k) &= 4\beta_k \sum_{\tilde{c}_m \in \tilde{\mathcal{C}}} \left[\exp \left\{ -\frac{S^2 |\tilde{c}_m|^2}{2\sigma^2} \right\} \mu_k(\tilde{c}_m) \times \right. \\ &\quad \cosh \left(\frac{S \Re\{\tilde{c}_m\} \Re\{y^*(k) e^{j(2\pi k \vartheta + \phi)}\}}{\sigma^2} + \frac{L_{2p}(k)}{2} \right) \times \\ &\quad \left. \cosh \left(\frac{S \Im\{\tilde{c}_m\} \Im\{y^*(k) e^{j(2\pi k \vartheta + \phi)}\}}{\sigma^2} - \frac{L_{2p-1}(k)}{2} \right) \right]. \end{aligned} \quad (3.41)$$

Recalling that $\tilde{\mathcal{C}} = \{(2i-1)d_p + j(2n-1)d_p\}_{i,n=1}^{2^{p-1}}$, the sum over $\tilde{c}_m \in \tilde{\mathcal{C}}$ in (3.41) can be

written as a double sum over the counters i and n after replacing \tilde{c}_m by $(2i-1)d_p + j(2n-1)d_p$.

Therefore, in order to factor $D_{\alpha}(k)$, the term $\mu_k(\tilde{c}_m = (2i-1)d_p + j(2n-1)d_p)$ must be factored

into two terms, one depending only on i and the other only on n . Here, we are actually dealing

with the remaining $2p - 2$ MSBs, $\bar{b}_1^m \bar{b}_2^m \bar{b}_3^m \cdots \bar{b}_{l-1}^m \bar{b}_{l+1}^m \cdots \bar{b}_{2p-5}^m \bar{b}_{2p-4}^m \bar{b}_{2p-3}^m \bar{b}_{2p-2}^m$. Hence, since the two LSBs \bar{b}_{2p-1}^m and

\bar{b}_{2p}^m are not involved in $\mu_k(\tilde{c}_m)$ (and are the same² for all $\tilde{c}_m \in \tilde{\mathcal{C}}_p$

³ they will be represented by “ $\times \times$ ” in (3.1), i.e. :

$$\tilde{c}_m \longleftrightarrow \underbrace{\bar{b}_1^m \bar{b}_2^m \cdots \bar{b}_l^m \cdots \bar{b}_{2p-5}^m \bar{b}_{2p-4}^m}_{\bar{b}_p^m} \bar{b}_{2p-3}^m \bar{b}_{2p-2}^m \times \times. \quad (3.42)$$

In addition, as highlighted in (3.42), it will prove very useful to represent the first $2p - 4$ MSBs

by the shorthand notation \bar{b}_p^m , i.e., $\bar{b}_p^m \triangleq \bar{b}_1^m \bar{b}_2^m \cdots \bar{b}_l^m \cdots \bar{b}_{2p-5}^m \bar{b}_{2p-4}^m$. For more convenience, we

will rather use the superscript (i, n) instead of m in (3.42) since $\tilde{c}_m = (2i-1)d_p + j(2n-1)d_p$.

That is :

$$\tilde{c}_m \longleftrightarrow \bar{b}_p^{(i,n)} \bar{b}_{2p-3}^{(i,n)} \bar{b}_{2p-2}^{(i,n)} \times \times. \quad (3.43)$$

2. The values of these two LSBs are defined according to the top-right quadrant of the basic Gray-coded QPSK constellation used in “step 3” during the recursive construction algorithm. For instance, in the example depicted in Fig. 3.1, they will be “ $\times \times = 11$ ”.

3. Actually $\tilde{\mathcal{C}}_p = \tilde{\mathcal{C}}$, but later on we have to make a difference between $\tilde{\mathcal{C}}$ in a 2^{2p} -QAM and when considering a $2^{2(p-1)}$ -QAM.

Using this mapping, all the points of the top-right quadrant of the obtained 2^{2p} -QAM constellation are graphically represented in Fig. 3.2 where the bits $\bar{b}_{2p-1}^{(i,n)}$ and $\bar{b}_{2p}^{(i,n)}$ are being assigned their true values. Each symbol \tilde{c}_m in $\tilde{\mathcal{C}}_p$ which has coordinates $((2i - 1)d_p, (2n - 1)d_p)$ in the current 2^{2p} -QAM constellation (x - axis and y - axis in Fig. 3.2) has already different coordinates (a', b') in the original $2^{2(p-1)}$ -QAM constellation (x' - axis and y' - axis in Fig. 3.2); associated with a symbol $c_{m'} = a' + jb'$ in \mathcal{C}_{p-1} . By inspecting Fig 3.2, it can be shown that

$$c_{m'} = (2i - 1 - 2^{p-1})d_p + j(2n - 1 - 2^{p-1})d_p. \quad (3.44)$$

Moreover, we have the following result :

$$c_{m'} \longleftrightarrow \bar{\mathbf{b}}_p^{(i,n)} \bar{b}_{2p-3}^{(i,n)} \bar{b}_{2p-2}^{(i,n)}. \quad (3.45)$$

since the first $2p - 2$ MSBs of each symbol $\tilde{c}_m \in \tilde{\mathcal{C}}_p$ are obtained (during “step 1”) from the whole bit sequence of the symbol $c_{m'}$ associated to it in the original $2^{2(p-1)}$ -QAM constellation.

From (3.34), we have :

$$\begin{aligned} \mu_{k,p}(\tilde{c}_m) &\triangleq \gamma_k(\bar{\mathbf{b}}_p^{(i,n)}) \exp \left\{ (2\bar{b}_{2p-3}^{(i,n)} - 1)L_{2p-3}(k)/2 \right\} \times \\ &\quad \exp \left\{ (2\bar{b}_{2p-2}^{(i,n)} - 1)L_{2p-2}(k)/2 \right\}, \end{aligned} \quad (3.46)$$

where

$$\gamma_k(\bar{\mathbf{b}}_p^{(i,n)}) \triangleq \prod_{l=1}^{2(p-1)-2} \exp \left\{ (2\bar{b}_l^{(i,n)} - 1)L_{2p-2}(k)/2 \right\}, \quad (3.47)$$

On the other hand, denoting the top-right quadrant of the original $2^{2(p-1)}$ -QAM constellation

by $\tilde{\mathcal{C}}_{p-1}$, it also holds $\mathcal{C}_{p-1} = \tilde{\mathcal{C}}_{p-1} \cup (-\tilde{\mathcal{C}}_{p-1}) \cup \tilde{\mathcal{C}}_{p-1}^* \cup (-\tilde{\mathcal{C}}_{p-1}^*)$. Then, for some $\tilde{c}_{m'} \in \mathcal{C}_{p-1}$, we have

$c_{m'} \in \{\tilde{c}_{m'}, -\tilde{c}_{m'}, \tilde{c}_{m'}^*, -\tilde{c}_{m'}^*\}$. In turn, the symbols $c_{m'}$ themselves are obtained from a previous

Gray-coded $2^{2(p-2)}$ -QAM constellation by applying the same recursive construction algorithm.

Therefore, due to symmetries of “step 2” it follows that $\tilde{c}_{m'}$, $-\tilde{c}_{m'}$, $\tilde{c}_{m'}^*$, and $-\tilde{c}_{m'}^*$ have the same

$2p-4$ MSBs which are represented by $\bar{\mathbf{b}}_p^{(i,n)}$. Consequently, according to the definition of (3.34),

we have $\gamma_k(\bar{\mathbf{b}}_p^{(i,n)}) = \mu_{k,p-1}(\tilde{c}_{m'})$ thereby yielding the following recursive property :

$$\begin{aligned} \mu_{k,p}(\tilde{c}_m) &\triangleq \mu_{k,p-1}(\tilde{c}_{m'}) \exp \left\{ (2\bar{b}_{2p-3}^{(i,n)} - 1)L_{2p-3}(k)/2 \right\} \times \\ &\quad \exp \left\{ (2\bar{b}_{2p-2}^{(i,n)} - 1)L_{2p-2}(k)/2 \right\}. \end{aligned} \quad (3.48)$$

Actually one needs to express the bits $\bar{b}_{2p-3}^{(i,n)}$ and $\bar{b}_{2p-2}^{(i,n)}$ explicitly as function of i and n if $\mu_{k,p}(\tilde{c}_m)$

is to be factorized in terms of these two counters separately. This useful result is given by the

following lemma.

Lemma : The two bits $\bar{b}_{2p-3}^{(i,n)}$ and $\bar{b}_{2p-2}^{(i,n)}$ are expressed as :

$$\begin{aligned} \bar{b}_{2p-2}^{(i,n)} &= \left\lfloor \frac{i-1}{2^{p-2}} \right\rfloor \text{ and } \bar{b}_{2p-3}^{(i,n)} = \left\lfloor \frac{n-1}{2^{p-2}} \right\rfloor \\ &\forall i, n = 1, 2, \dots, 2^{p-1}. \end{aligned} \quad (3.49)$$

In (3.49), $\lfloor x \rfloor$ is the floor function which returns the largest integer which is smaller than or

equal to x .

Thus, injecting (3.49) in (3.48), it follows :

$$\begin{aligned} \mu_{k,p}(\tilde{c}_m) &\triangleq \mu_{k,p-1}(\tilde{c}_{m'}) \exp \left\{ \left(2 \lfloor \frac{n-1}{2^{p-2}} \rfloor - 1 \right) \frac{L_{2p-3}(k)}{2} \right\} \times \\ &\quad \exp \left\{ \left(2 \lfloor \frac{i-1}{2^{p-2}} \rfloor - 1 \right) \frac{L_{2p-2}(k)}{2} \right\}. \end{aligned} \quad (3.50)$$

Following the same reasoning from (3.42) through (3.49), $\mu_{k,p-1}(\tilde{c}_{m'})$ itself can be written in the same recursive form of (3.50) by considering the recursive reconstruction of $\tilde{\mathcal{C}}_{p-1}$ (highlighted in blue color in Fig 3.2) from the $2^{2(p-2)}$ -QAM constellation. Consequently, by repeating this process down constellations, it can be shown that $\mu_k(\tilde{c}_m)$ is factored into two independent terms one depending on i only and the other on n only as follows :

$$\mu_k(\tilde{c}_m) = \theta_{k,2p}(i)\theta_{k,2p-1}(n). \quad (3.51)$$

where the terms $\theta_{k,2p}(i)$ and $\theta_{k,2p-1}(n)$ are obtained recursively, for any $p \geq 2$, as follows :

$$\begin{aligned} \theta_{k,2p}(i) &= \theta_{k,2p-2} \left(\frac{|2i-1-2^{p-1}|+1}{2} \right) \times \\ &\quad \exp \left\{ \left(2 \lfloor \frac{i-1}{2^{p-2}} \rfloor - 1 \right) \frac{L_{2p-2}(k)}{2} \right\}, \end{aligned} \quad (3.52)$$

$$\begin{aligned} \theta_{k,2p-1}(n) &= \theta_{k,2p-3} \left(\frac{|2n-1-2^{p-1}|+1}{2} \right) \times \\ &\quad \exp \left\{ \left(2 \lfloor \frac{n-1}{2^{p-2}} \rfloor - 1 \right) \frac{L_{2p-3}(k)}{2} \right\}, \end{aligned} \quad (3.53)$$

The initialization for $p = 1$ (i.e., the basic 4-QAM constellation) is given by $\theta_{k,2}(\cdot) = \theta_{k,1}(\cdot) = 1$, since $\mu_k(\tilde{c}_m) = 1 \forall \tilde{c}_m \in \tilde{\mathcal{C}}_1$. Now plugging (3.52) and (3.53) in (3.41) and using the fact that

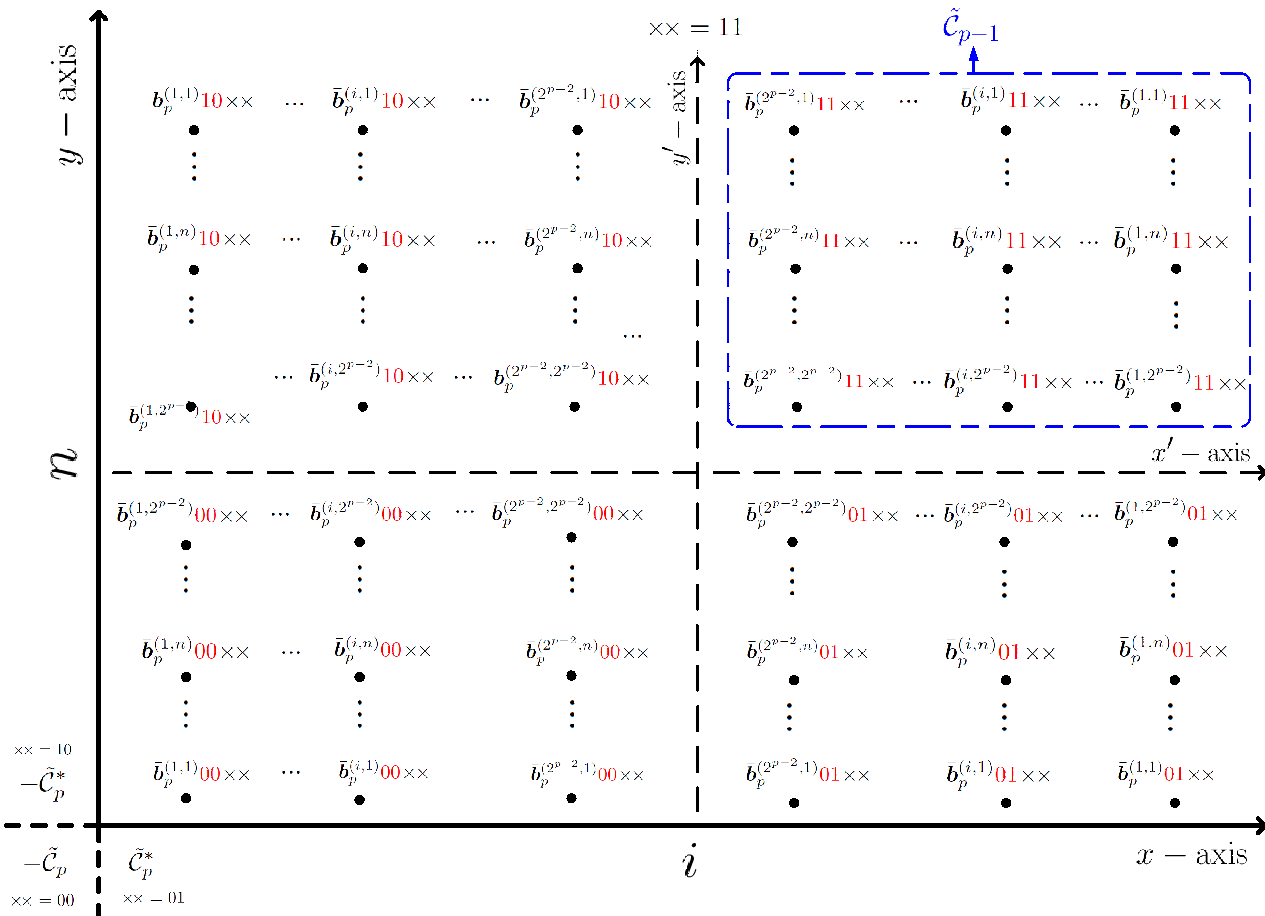


FIGURE 3.2 – Construction of Gray-coded Square-QAM constellations

$\tilde{\mathcal{C}}_p = \{(2i-1)d_p + j(2n-1)d_p\}_{i,n=1,2,\dots,2^{p-1}}$, the term $D_{\alpha}(k)$ is rewritten as follows :

$$\begin{aligned} D_{\alpha}(k) &= 4\beta_k \sum_{i=1}^{2^{p-1}} \sum_{n=1}^{2^{p-1}} \left[\exp \left\{ -\frac{S^2((2i-1)^2 + (2n-1)^2)d_p^2}{2\sigma^2} \right\} \right. \\ &\quad \theta_{k,2p}(i) \cosh \left(\frac{S(2i-1)d_p u(k)}{\sigma^2} + \frac{L_{2p}(k)}{2} \right) \times \\ &\quad \left. \theta_{k,2p-1}(n) \cosh \left(\frac{S(2n-1)d_p v(k)}{\sigma^2} - \frac{L_{2p-1}(k)}{2} \right) \right] \end{aligned} \quad (3.54)$$

where $u(k)$ and $v(k)$ are defined as $u(k) = \Re\{y^*(k)e^{j(2\pi k\vartheta+\phi)}\}$ and $v(k) = \Im\{y^*(k)e^{j(2\pi k\vartheta+\phi)}\}$.

Finally, splitting the two sums, it can be shown that $D_{\alpha}(k)$ is factorized as follows :

$$D_{\alpha}(k) = 4\beta_k F_{2p,\alpha}(u(k)) \times F_{2p-1,\alpha}(v(k)), \quad (3.55)$$

where $F_{q,\alpha}(\cdot)$ is given by :

$$\begin{aligned} F_{q,\alpha}(x) &= \sum_{i=1}^{2^{p-1}} \theta_{k,q}(i) \exp \left\{ -\frac{S^2(2i-1)^2 d_p^2}{2\sigma^2} \right\} \times \\ &\quad \cosh \left(\frac{S(2i-1)d_p x}{\sigma^2} + (-1)^q \frac{L_q(k)}{2} \right), \end{aligned} \quad (3.56)$$

where the counter q is used, from now on, to refer to $2p$ or $2p-1$ depending on the context.

The factorization of $D_{\alpha}(k)$ in (3.55) will prove very useful in deriving the analytical expressions of the considered stochastic CRLBs. In fact, by injecting (3.55) back into (3.28) the LLF for

arbitrary square-QAM constellation becomes as follows :

$$\begin{aligned} L_y(\alpha) = & -\frac{1}{2\sigma^2} \sum_{k=k_0}^{k_0+K-1} \left(I(k)^2 + Q(k)^2 \right) + \sum_{k=k_0}^{k_0+K-1} \ln \{ F_{2p,\alpha}(u(k)) \} \\ & + \sum_{k=k_0}^{k_0+K-1} \ln \{ F_{2p-1,\alpha}(v(k)) \}, \end{aligned} \quad (3.57)$$

involving thereby the sum of two analogous terms (the two last sums). Now, we further show that $U(k)$ and $V(k)$ (whose realizations are $u(k)$ and $v(k)$, respectively) are two independent random variables which are *almost* identically distributed (i.e., their pdfs have the same structure, but are parameterized differently) . In fact, injecting (3.54) in (3.25) and using the fact that $I(k)^2 + Q(k)^2 = u(k)^2 + v(k)^2$, it can be shown that $p(y(k); \boldsymbol{\alpha})$ factorized as follows :

$$p(y(k); \boldsymbol{\alpha}) = p(u(k); \boldsymbol{\alpha})p(v(k); \boldsymbol{\alpha}), \quad (3.58)$$

where

$$p(u(k); \boldsymbol{\alpha}) = \frac{2\beta_{k,2p}}{\sqrt{2\pi\sigma^2}} \exp \left\{ -\frac{u(k)^2}{2\sigma^2} \right\} F_{2p,\alpha}(u(k)), \quad (3.59)$$

$$p(v(k); \boldsymbol{\alpha}) = \frac{2\beta_{k,2p-1}}{\sqrt{2\pi\sigma^2}} \exp \left\{ -\frac{v(k)^2}{2\sigma^2} \right\} F_{2p-1,\alpha}(v(k)), \quad (3.60)$$

with

$$\beta_{k,2p} = \frac{1}{2^p} \prod_{l=1}^p \operatorname{sech} \left(\frac{L_{2l}(k)}{2} \right) \quad (3.61)$$

$$\beta_{k,2p-1} = \frac{\beta_k}{\beta_{k,2p}}. \quad (3.62)$$

Moreover, we have $p(u(k), v(k); \boldsymbol{\alpha}) = p(y(k)^* e^{j(2\pi k\nu + \phi)}; \boldsymbol{\alpha})$ since $u(k)$ and $v(k)$ are indeed the real and imaginary parts of $y(k)^* e^{j(2\pi k\nu + \phi)}$. Then, since $e^{j(2\pi k\nu + \phi)}$ is assumed to be deterministic, we have $p(y(k)^* e^{j(2\pi k\nu + \phi)}; \boldsymbol{\alpha}) = p(y(k); \boldsymbol{\alpha})$. Therefore, using (3.58) we obtain :

$$p(u(k), v(k); \boldsymbol{\alpha}) = p(u(k); \boldsymbol{\alpha})p(v(k); \boldsymbol{\alpha}). \quad (3.63)$$

meaning that the joint distribution of $U(k)$ and $V(k)$ is factored and hence they are two independent random variables which are *almost* distributed according to (3.59) and (3.60).

Chapitre 4

Derivation of the CRLB Analytical Expressions

4.1 CRLB for coded SNR estimation [43]

We begin first by deriving the FIM elements using the LLF expressions obtained in the previous section. We consider the case of square-QAM-modulated signals since it is the most general one. Equivalent derivations can be applied in case of BPSK-, MSK- and QPSK-modulated-signals to obtain the corresponding FIM elements. We will also detail the derivations for the first FIM element only and the other ones can be obtained in the same way. To begin with and using

(3.57), we have the following result :

$$\begin{aligned} \mathbb{E}_{\boldsymbol{y}} \left\{ \frac{\partial^2 \ln(p(\boldsymbol{y}; \boldsymbol{\alpha}^{(1)}))}{\partial S^2} \right\} &= \sum_{k=0}^{K-1} \mathbb{E} \left\{ \frac{\partial^2 \ln(F_{2p, \boldsymbol{\alpha}^{(1)}}(u(k)))}{\partial S^2} \right\} \\ &\quad + \sum_{k=0}^{K-1} \mathbb{E} \left\{ \frac{\partial^2 \ln(F_{2p-1, \boldsymbol{\alpha}^{(1)}}(v(k)))}{\partial S^2} \right\}. \end{aligned} \quad (4.1)$$

As mentioned previously, the two terms in the right-hand side of (4.1) are analogous and they can be derived in the same way, especially because the RVs $U(k)$ and $V(k)$ are *almost* identically distributed. Thus, for ease of notations, we will henceforth use $z_q(k)$ to refer to $u(k)$ when $q = 2p$ and to $v(k)$ when $q = 2p - 1$, respectively. Using this generic notation and if we denote :

$$\begin{aligned} \dot{F}_{q, \boldsymbol{\alpha}^{(1)}}(z_q(k)) &\triangleq \frac{\partial F_{q, \boldsymbol{\alpha}^{(1)}}(z_q(k))}{\partial S}, \\ \ddot{F}_{q, \boldsymbol{\alpha}^{(1)}}(z_q(k)) &\triangleq \frac{\partial^2 F_{q, \boldsymbol{\alpha}^{(1)}}(z_q(k))}{\partial S^2}, \end{aligned}$$

it can be shown that :

$$\mathbb{E} \left\{ \frac{\partial^2 \ln(F_{q, \boldsymbol{\alpha}^{(1)}}(z_q(k)))}{\partial S^2} \right\} = \mathbb{E} \left\{ \frac{\ddot{F}_{q, \boldsymbol{\alpha}^{(1)}}(z_q(k))}{F_{q, \boldsymbol{\alpha}^{(1)}}(z_q(k))} \right\} - \mathbb{E} \left\{ \frac{\dot{F}_{q, \boldsymbol{\alpha}^{(1)}}(z_q(k))^2}{F_{q, \boldsymbol{\alpha}^{(1)}}(z_q(k))^2} \right\}.$$

The second expectation is obtained by integrating over the distribution of $z_q(k)$ obtained earlier in (3.59) and (3.60) for $q = 2p$ and $q = 2p - 1$, respectively :

$$\begin{aligned} \mathbb{E} \left\{ \frac{\dot{F}_{q, \boldsymbol{\alpha}^{(1)}}(z_q(k))^2}{F_{q, \boldsymbol{\alpha}^{(1)}}(z_q(k))^2} \right\} &= \int_{-\infty}^{+\infty} \frac{\dot{F}_{q, \boldsymbol{\alpha}^{(1)}}(z_q(k))^2}{F_{q, \boldsymbol{\alpha}^{(1)}}(z_q(k))^2} p(z_q(k), \boldsymbol{\alpha}^{(1)}) dz_q(k) \\ &= \frac{2\beta_{k,q}}{\sqrt{2\pi}\sigma^2} \int_{-\infty}^{+\infty} \frac{\dot{F}_{q, \boldsymbol{\alpha}^{(1)}}(z_q(k))^2}{F_{\boldsymbol{\alpha}^{(1)}}(z_q(n))} e^{-\frac{z_q(n)^2}{2\sigma^2}} dz_q(n). \end{aligned} \quad (4.2)$$

We further simplify (4.2) by changing $z_q(k)/\sigma$ by t and using $\rho = S^2/2\sigma^2$ to obtain :

$$\mathrm{E} \left\{ \frac{\dot{F}_{q,\alpha^{(1)}}(z_q(k))^2}{F_{q,\alpha^{(1)}}(z_q(k))^2} \right\} = \frac{2\beta_{k,q}d_p^2}{\sigma^2} \psi_{k,q}(\rho), \quad (4.3)$$

in which $\Psi_{k,q}(\rho)$ is defined as :

$$\Psi_{k,q}(\rho) \triangleq \frac{1}{\sqrt{2\pi}} \int_{-\infty}^{+\infty} \frac{\lambda_{k,q}(\rho, t)^2}{\delta_{k,q}(\rho, t)} e^{-\frac{t^2}{2}} dt, \quad (4.4)$$

where, by using $\omega_{k,q}(i) \triangleq \theta_{k,q}(i) e^{-(2i-1)^2 d_p^2 \rho}$, the functions $\delta_{k,q}(\cdot, \cdot)$ and $\lambda_{k,q}(\cdot, \cdot)$ are, respectively,

given by (4.5) and (4.6) :

$$\delta_{k,q}(\rho, t) = \sum_{i=1}^{2p-1} \omega_{k,q}(i) \cosh \left(\sqrt{2\rho} (2i-1)d_p t + \frac{(-1)^q L_q(k)}{2} \right), \quad (4.5)$$

$$\begin{aligned} \lambda_{k,q}(\rho, t) = & \sum_{i=1}^{2p-1} (2i-1)^2 \omega_{k,q}(i) \left[t \sinh \left(\sqrt{2\rho} (2i-1)d_p t + \frac{(-1)^q L_q(k)}{2} \right) \right. \\ & \left. - d_p (2i-1) \sqrt{2\rho} \cosh \left(\sqrt{2\rho} (2i-1)d_p t + \frac{(-1)^q L_q(k)}{2} \right) \right]. \end{aligned} \quad (4.6)$$

In addition, after tedious algebraic manipulations, we show the following identity :

$$\mathrm{E} \left\{ \frac{\ddot{F}_{q,\alpha^{(1)}}(z_q(k))}{F_{q,\alpha^{(1)}}(z_q(k))} \right\} = 0. \quad (4.7)$$

Therefore, by using $\alpha_{k,q} \triangleq 2\beta_{k,q}d_p^2 \psi_{k,q}(\rho)$ and injecting (4.3) for $q = 2p$ and $q = 2p-1$ in (4.24),

it follows :

$$\mathrm{E}_{\mathbf{y}} \left\{ \frac{\partial^2 \ln(p(\mathbf{y}; \boldsymbol{\alpha}^{(1)}))}{\partial S^2} \right\} = -\frac{1}{\sigma^2} \sum_{k=0}^{K-1} \left[\alpha_{k,2p} + \alpha_{k,2p-1} \right] \quad (4.8)$$

Equivalent algebraic manipulations lead to the following analytical expressions for the second FIM diagonal element :

$$\mathbb{E}_{\mathbf{y}} \left\{ \frac{\partial^2 \ln(p(\mathbf{y}; \boldsymbol{\alpha}^{(1)}))}{\partial \sigma^2 \partial S} \right\} = \frac{K}{\sigma^4} + \frac{1}{\sigma^4} \sum_{k=0}^{K-1} \left[\nu_{k,2p} + \nu_{k,2p-1} \right], \quad (4.9)$$

where $\nu_{k,q}$ (for $q = 2p$ or $2p - 1$) is given by :

$$\nu_{k,q} = c_{4,q}^{(k)} \rho^2 + 2 \left(c_{2,q}^{(k)} - 2\beta_{k,q} d_p^2 \Phi_{q,k}(\rho) \right) - c_{0,q}^{(k)}. \quad (4.10)$$

The coefficients $c_{l,q}^{(k)}$ are given by :

$$c_{l,q}^{(k)} = 2\beta_{k,q} d_p^l \cosh(L_q(k)/2) \sum_{i=1}^{2p-1} \theta_{k,q}(i) (2i-1)^l, \quad (4.11)$$

and the function $\Phi_{k,q}(\cdot)$ is defined as :

$$\Phi_{k,q}(\rho) \triangleq \frac{1}{\sqrt{2\pi}} \int_{-\infty}^{+\infty} \frac{\gamma_{k,q}^2(\rho, t)}{\delta_{k,q}(\rho, t)} e^{-\frac{t^2}{2}} dt \quad (4.12)$$

with $\gamma_{k,q}(\cdot, \cdot)$ being given by :

$$\begin{aligned} \gamma_{k,q}(\rho, t) = & \sum_{i=1}^{2p-1} (2i-1)^2 \omega_{k,q}(i) \left[t \sinh \left(\sqrt{2\rho} (2i-1)d_p t + \frac{(-1)^q L_q(k)}{2} \right) \right. \\ & \left. - d_p (2i-1) \sqrt{\frac{\rho}{2}} \cosh \left(\sqrt{2\rho} (2i-1)d_p t + \frac{(-1)^q L_q(k)}{2} \right) \right]. \end{aligned} \quad (4.13)$$

Equivalent derivations also yield the following expression for the off-diagonal element of $\mathbf{I}(\boldsymbol{\alpha}^{(1)})$:

$$\mathbb{E}_{\mathbf{y}} \left\{ \frac{\partial^2 \ln(p(\mathbf{y}; \boldsymbol{\alpha}^{(1)}))}{\partial \sigma^2 \partial S} \right\} = -\frac{S}{\sigma^4} \sum_{k=0}^{K-1} \left[\eta_{k,2p} + \eta_{k,2p-1} \right], \quad (4.14)$$

in which $\eta_{k,q} \triangleq c_{2,q}^{(k)} - 2d_p^2 \beta_{k,q} \Omega_{k,q}(\rho)$ with the function $\Omega_{k,q}(.)$ being defined as :

$$\Omega_{k,q}(\rho) \triangleq \frac{1}{\sqrt{2\pi}} \int_{-\infty}^{+\infty} \frac{\gamma_{q,\rho}(t)\lambda_{q,\rho}(t)}{\delta_{q,\rho}(t)} e^{-\frac{t^2}{2}} dt \quad (4.15)$$

Therefore, from (4.8), (4.9) and (4.14), the global Fisher information matrix decomposes into the sum of elementary FIMs :

$$\mathbf{I}(\boldsymbol{\alpha}^{(1)}) = \sum_{k=0}^{K-1} \mathbf{I}_k(\boldsymbol{\alpha}^{(1)}) \quad (4.16)$$

where $\{\mathbf{I}_k(\boldsymbol{\alpha}^{(1)})\}_{k=0}^{K-1}$ is the FIM pertaining to the estimation of the SNR from the received sample $y(k)$ alone :

$$\mathbf{I}_k(\boldsymbol{\alpha}^{(1)}) = \frac{1}{\sigma^4} \begin{pmatrix} \sigma^2 [\alpha_{k,2p} + \alpha_{k,2p-1}] & S[\eta_{k,2p} + \eta_{k,2p-1}] \\ & \\ S[\eta_{k,2p} + \eta_{k,2p-1}] - [\nu_{2p,k} + \nu_{2p-1,k} + 1] & \end{pmatrix}. \quad (4.17)$$

This FIM expression in the general case of a coded-aided estimation corroborates the two traditional extreme cases of completely NDA and completely DA estimations. Indeed, in the former case, no *a priori* information about the bits is available at the receiver and, hence, $P[b_l^k = 1] = P[b_l^k = 0] = 1/2$ meaning that $L_l^{\text{NDA}}(k) = 0$. In the latter case, however, the bits are *a priori* perfectly known and, therefore, at the receiver side we have $\{P[b_l^k = 1] = 1 \text{ hence } P[b_l^k = 0] = 0\}$ or $\{P[b_l^k = 0] = 1 \text{ hence } P[b_l^k = 1] = 0\}$ and consequently the LLRs verify : $L_l^{\text{DA}}(k) = \pm\infty$. Injecting $L_l^{\text{NDA}}(k)$ and $L_l^{\text{DA}}(k)$ in the entries of $\mathbf{I}_k(\boldsymbol{\alpha})$, and recognizing

some easy simplifications lead to the exact same expression for the FIMs developed earlier in [23] in the NDA and DA cases, respectively.

Now, since the inverse of any (2×2) matrix is directly obtained by swapping the two diagonal elements and negating the off-diagonal ones, it can be shown from (4.16) that :

$$\mathbf{I}(\boldsymbol{\alpha}^{(1)})^{-1} = \sum_{k=0}^{K-1} \frac{\det \{\mathbf{I}_k(\boldsymbol{\alpha}^{(1)})\}}{\det \{\mathbf{I}(\boldsymbol{\alpha}^{(1)})\}} \mathbf{I}_k(\boldsymbol{\alpha}^{(1)})^{-1}, \quad (4.18)$$

where $\det \{\cdot\}$ returns the determinant of any square matrix. Finally, injecting (4.18) and (2.8) in (2.7), it can be shown be shown that :

$$\text{CRLB}(\rho) = \sum_{k=0}^{K-1} \omega(k) \text{CRLB}_k(\rho), \quad (4.19)$$

where $\omega(k) = \det \{\mathbf{I}_k(\boldsymbol{\alpha}^{(1)})\} / \det \{\mathbf{I}(\boldsymbol{\alpha}^{(1)})\}$ and $\text{CRLB}_k(\rho)$, given by (4.20) on the top of the next page, is the elementary CRLB pertaining to the estimation of the SNR given the received sample $y(k)$ only. The higher the weighting coefficient, $\omega(k)$, the more $y(k)$ contributes to the overall achievable performance. These coefficients are not equal since the received samples are not identically distributed. This is in contrast to the NDA or DA estimation scenarios where all the samples are indeed identically distributed. This yields identical elementary FIMs and equal weighting coefficients leading thereby to a the factor K in the overall CRLB as shown in [23].

$$\text{CRLB}_k(\rho) = \frac{100}{\ln(10)^2 \rho} \frac{2(\nu_{2p,k}(\rho) + \nu_{2p-1,k}(\rho) + 1) - (4\eta_{2p,k}(\rho) + 4\eta_{2p-1,k}(\rho) + \alpha_{2p,k}(\rho) + \alpha_{2p-1,k}(\rho))\rho}{(\nu_{2p,k}(\rho) + \nu_{2p-1,k}(\rho) + 1)(\alpha_{2p,k}(\rho) + \alpha_{2p-1,k}(\rho)) - 2(\eta_{2p,k}(\rho) + \eta_{2p-1,k}(\rho))\rho}, \quad (4.20)$$

Equivalent derivations lead to the following simple CRLB expression in case of a BPSK or MSK signals (exactly the same expression for both modulations) :

$$\text{CRLB}(\rho) = \frac{100}{\ln^2(10)K\rho} \frac{\rho[H(\rho) - K] - 2K}{[1 + 2\rho]H(\rho) - K} \quad (4.21)$$

where

$$H(\rho) = \frac{e^{-\rho}}{\sqrt{2\pi}} \sum_{k=0}^{K-1} \frac{h_k(\rho)}{\cosh(L(k)/2)}, \quad (4.22)$$

with

$$h_k(\rho) = h_0(\rho) = \int_{-\infty}^{+\infty} \frac{t^2 e^{-\frac{t^2}{2}}}{\cosh(\sqrt{2\rho}t + L(k)/2)} dt. \quad (4.23)$$

Again, it can be easily verified that, when $L(k) = 0$, [4.21] yields exactly the same expression for NDA CRLB of BPSK signals derived earlier in 21. The CRLB for QPSK signals can be obtained as a special case of square QAM signals by taking $p = 1$. Finally, in order to evaluate the different CRLBs derived in this paper, the LLRs of the bits must be computed. Fortunately, owing to the turbo decoding principle, it was shown [8] that the *extrinsic* information of the bits which is delivered, during the decoding process, is an accurate estimate of these LLRs.

4.2 CRLB for coded phase and CFO estimation [44]

Actually, using (3.57), it can be shown that :

$$\begin{aligned} \mathbb{E}_{\mathbf{y}} \left\{ \frac{\partial^2 \ln(p(\mathbf{y}; \boldsymbol{\alpha}^{(2)}))}{\partial \phi^2} \right\} &= \sum_{k=k_0}^{k_0+K-1} \mathbb{E} \left\{ \frac{\partial^2 \ln(F_{2p, \boldsymbol{\alpha}^{(2)}}(u(k)))}{\partial \phi^2} \right\} \\ &+ \sum_{k=k_0}^{k_0+K-1} \mathbb{E} \left\{ \frac{\partial^2 \ln(F_{2p-1, \boldsymbol{\alpha}^{(2)}}(-v(k)))}{\partial \phi^2} \right\}. \end{aligned} \quad (4.24)$$

Using the distribution of $U(k)$ and $V(k)$, and the definition $\mathbb{E} \left\{ \frac{\partial^2 \ln(F_{q, \boldsymbol{\alpha}^{(2)}}(u(k)))}{\partial \phi^2} \right\} \triangleq \eta_{q,k}(\rho)$, we

were able to show that :

$$\eta_{q,k}(\rho) = A_{q,k} \rho \left(A_{q,k} \rho - 4\beta_{k,q} d_p^2 \Psi_q(\rho) \left(\frac{1}{A_{q,k}} + \rho \right) \right), \quad (4.25)$$

where

$$A_{q,k} = 4\beta_{k,q} \cosh \left(\frac{L_q(k)}{2} \right) d_p^2 \sum_{i=1}^{2^p-1} \theta_{k,q}(i) (2i-1)^2 \quad (4.26)$$

$$\Psi_q(\rho) = \frac{1}{\sqrt{2\pi}} \int_{-\infty}^{+\infty} \frac{\lambda_{q,\rho}^2(t)}{\delta_{q,\rho}(t)} e^{-\frac{t^2}{2}} dt \quad (4.27)$$

with

$$\begin{aligned} \lambda_{q,\rho}(t) &= \sum_{i=1}^{2^p-1} (2i-1) \theta_{k,q}(i) e^{-(2i-1)^2 d_p^2 \rho} \sinh(h_{i,q}(t)), \\ \delta_{q,\rho}(t) &= \sum_{i=1}^{2^p-1} \theta_{k,q}(i) e^{-(2i-1)^2 d_p^2 \rho} \cosh(h_{i,q}(t)), \end{aligned} \quad (4.28)$$

where, $h_{i,q}(t) = \sqrt{2\rho}(2i-1)d_p t + (-1)^q \frac{L_q(k)}{2}$. Finally, plugging (4.25) into (4.24), the first diagonal element follows immediately as :

$$\mathbb{E}_{\mathbf{Y}} \left\{ \frac{\partial^2 \ln(P(\mathbf{y}; \boldsymbol{\theta}))}{\partial \phi^2} \right\} = \sum_{k=k_0}^{k_0+K-1} (\eta_{2p,k}(\rho) + \eta_{2p-1,k}(\rho)). \quad (4.29)$$

Using equivalent manipulations to derive the other elements of $\mathbf{I}(\boldsymbol{\alpha}^{(2)})$, we obtain the following result :

$$[\mathbf{I}(\boldsymbol{\alpha}^{(2)})]_{i,j} = \sum_{k=k_0}^{k_0+K-1} (2k\pi)^{4-(i+j)} (\eta_{2p,k}(\rho) + \eta_{2p-1,k}(\rho)). \quad (4.30)$$

Therefore, the Fisher information matrix is given by :

$$\mathbf{I}(\boldsymbol{\alpha}^{(2)}) = \sum_{k=k_0}^{k_0+K-1} \begin{pmatrix} (2\pi)^2 k^2 B_k(\rho) & 2\pi k B_k(\rho) \\ 2\pi k B_k(\rho) & B_k(\rho) \end{pmatrix}, \quad (4.31)$$

with

$$B_k(\rho) = \eta_{2p,k}(\rho) + \eta_{2p+1,k}(\rho). \quad (4.32)$$

This general FIM expression in the case of coded transmissions corroborate the special case of non-data-aided estimation, where all the transmitted information are equally likely ($P[b_i^k] = \frac{1}{2}$) implying $L_l(k) = 0$). Easy simplifications using $L_l(k)$ lead to the exact same expression of the FIM for the NDA case. Finally, using the fact that the FIM is (2x2) dimensional, The CRLB

for the joint carrier phase and CFO estimation is then given by (whitout loss of generality, we suppose that k_0 and $k_0 + K - 1$ are even numbers) :

$$\begin{aligned}
\text{CRLB}(\alpha_i^{(2)}) &= [\mathbf{I}^{-1}(\boldsymbol{\alpha}^{(2)})]_{i,i} \\
&= \left(\sum_{k=\frac{k_0}{2}}^{\frac{k_0+K-1}{2}} \underbrace{I_k(\boldsymbol{\alpha}^{(2)}) + I_{k+1}(\boldsymbol{\alpha}^{(2)})}_{J_k} \right)_{i,i}^{-1} \\
&= \left(\sum_{k=\frac{k_0}{2}}^{\frac{k_0+K-1}{2}} [J_k(\boldsymbol{\alpha}^{(2)})^{-1}]_{i,i} \frac{\det J_k(\boldsymbol{\alpha}^{(2)})}{\det I(\boldsymbol{\alpha}^{(2)})} \right) \\
&= \sum_{k=\frac{k_0}{2}}^{\frac{k_0+K-1}{2}} \text{CRLB}_{k,k+1}(\alpha_i^{(2)}) \left[\frac{\det J_k(\boldsymbol{\alpha}^{(2)})}{\det I(\boldsymbol{\alpha}^{(2)})} \right], \tag{4.33}
\end{aligned}$$

where $I(\boldsymbol{\alpha}^{(2)})$ is the FIM based on the single received sample $y(k)$, and $\text{CRLB}_{k,k+1}(\alpha_i^{(2)})$ is the CRLB of $\alpha_i^{(2)}$ based on the two received samples $y(k), y(k+1)$. This decomposition is straightforward since the FIM is 2x2, and each of the considered matrices is invertible. and is given by :

$$\text{CRLB}_{k,k+1}(\alpha_i^{(2)}) = \frac{N_{i,k}(\rho)}{D_k(\rho)}, \tag{4.34}$$

where

$$N_{i,k}(\rho) = (2\pi k)^{4-2i} B_k(\rho) + (2\pi(k+1))^{4-2i} B_{k+1}(\rho), \tag{4.35}$$

$$\begin{aligned}
D_k(\rho) &= [(2\pi k)^2 B_k(\rho) + (2\pi(k+1))^2 B_{k+1}(\rho)][B_k(\rho) + \\
&\quad B_{k+1}(\rho)] - [(2\pi k)B_k(\rho) + (2\pi(k+1))B_{k+1}(\rho)]^2. \\
&\tag{4.36}
\end{aligned}$$

From (4.33), we see that the CRLB of the phase and CFO estimation based on the received samples vector $\mathbf{y} = [y(k_0), y(k_0 + 1), \dots, y(k_0 + K - 1)]^T$ is the summation of the elementary CRLBs of each received two samples $(y(k), y(k+1))$ individually (this decomposition into sums of CRLBs is possible thanks to the approximation that the received samples are independent, due to the outer interleaver), weighted by the term $\frac{\det J_k(\boldsymbol{\alpha}^{(2)})}{\det I(\boldsymbol{\alpha}^{(2)})}$ (these weights are not equal since the received samples are independent but not identically distributed) which reflect the contribution of the estimation from the received the samples $y(k), y(k + 1)$ on the estimation based on the whole received vector \mathbf{y} :

$$\frac{\det J_{i_0}(\boldsymbol{\alpha}^{(2)})}{\det I(\boldsymbol{\alpha}^{(2)})} \ll 1 \Leftrightarrow \text{CRLB}(\rho) \simeq \sum_{k=\frac{k_0}{2}, k \neq \frac{k_0}{2}}^{\frac{k_0+K-1}{2}} \text{CRLB}_{k,k+1}(\rho) \quad (4.37)$$

In order to establish a closed-form expression of the CRLB for a given code structure (in our case a turbo code), we need to calculate the *a priori* probabilities of the coded bits involved in the expression of $\eta_{q,k}(\rho)$.

In the case of a BPSK or MSK modulation, the FIM matrix is the same and is given by :

$$I(\boldsymbol{\alpha}^{(2)}) = \begin{pmatrix} \sum_{k=k_0}^{k_0+K-1} (1 - h_k(\rho)) & \sum_{k=k_0}^{k_0+K-1} 2\pi k (1 - h_k(\rho)) \\ \sum_{k=k_0}^{k_0+K-1} 2\pi k (1 - h_k(\rho)) & \sum_{k=k_0}^{k_0+K-1} (2\pi)^2 k^2 (1 - h_k(\rho)) \end{pmatrix}, \quad (4.38)$$

where

$$h_k(\rho) = 2 \frac{e^{-\rho}}{\sqrt{2\pi} \cosh\left(\frac{L(k)}{2}\right)} \int_0^{+\infty} \frac{e^{-\frac{t^2}{2}}}{\cosh\left(\sqrt{2\rho}t + \frac{L(k)}{2}\right)} dt. \quad (4.39)$$

In the case of a NDA estimation, i.e. $L(k) = 0$, we have :

$$h_k(\rho) = h_0(\rho) = 2 \frac{e^{-\rho}}{\sqrt{2\pi}} \int_{-\infty}^{+\infty} \frac{e^{-\frac{t^2}{2}}}{\cosh\left(\sqrt{2\rho}t\right)} dt. \quad (4.40)$$

(4.41)

the FIM becomes :

$$I(\boldsymbol{\alpha}^{(2)}) = (1 - h_0(\rho)) \begin{pmatrix} K & \sum_{k=k_0}^{k_0+K-1} 2\pi k \\ \sum_{k=k_0}^{k_0+K-1} 2\pi k & \sum_{k=k_0}^{k_0+K-1} (2\pi)^2 k^2 \end{pmatrix}, \quad (4.42)$$

and the CRLB expression becomes the same as given in [22].

4.2.1 Empirical Evaluation of the CRLB

In this section, we develop an empirical procedure that evaluates the considered CRLBs through extensive Monte-Carlo simulations. These empirical CRLBs are used to validate our new analytical expressions. In fact, the CRLB can be expressed in terms of the symbols' *a posteriori* probabilities (APPs). We will also rely on another definition for the FIM elements which involves the first derivatives of the LLF instead of its second derivatives. In fact, as shown in [27],

the FIM elements can be written in the following equivalent form :

$$\mathbf{I}_{i,j}(\boldsymbol{\alpha}) = \text{E} \left(\frac{\partial \ln(p(\mathbf{y}; \boldsymbol{\alpha}))}{\partial \alpha_i} \frac{\partial \ln(p(\mathbf{y}; \boldsymbol{\alpha}))}{\partial \alpha_j} \right) \quad (4.43)$$

where

$$\ln(p(\mathbf{y}; \boldsymbol{\alpha})) = \ln \left(\sum_{i=1}^{M^K} P_i[\mathbf{x}] p(\mathbf{y} | \mathbf{x} = \mathbf{c}_i) \right), \quad (4.44)$$

is another formulation for the LLF in which $P_i[\mathbf{x}] = \text{Pr}\{\mathbf{x} = \mathbf{c}_i\}$ with $\mathbf{x} = [x(k_0), x(k_0 + 1), \dots, x(k_0 + K - 1)]$ being a vector that contains the *actual* sequence of transmitted symbols and $\{\mathbf{c}_i\}_{i=1}^{M^K}$ are all the *possible* sequences of coded symbols. Differentiating (4.44) with respect α_i leads to the following expression :

$$\frac{\partial \ln(p(\mathbf{y}; \boldsymbol{\alpha}))}{\partial \alpha_i} = \sum_{i=1}^{M^K} \frac{P_i[\mathbf{x}] p(\mathbf{y} | \mathbf{x} = \mathbf{c}_i)}{p(\mathbf{y}; \boldsymbol{\alpha})} \times \frac{\partial \ln(p(\mathbf{y} | \mathbf{x} = \mathbf{c}_i))}{\partial \alpha_i}. \quad (4.45)$$

(4.46)

Then, owing to the Bayes' formula :

$$\frac{P_i[\mathbf{x}] p(\mathbf{y} | \mathbf{x} = \mathbf{c}_i)}{p(\mathbf{y}; \boldsymbol{\alpha})} = P(\mathbf{x} = \mathbf{c}_i | \mathbf{y}), \quad (4.47)$$

the right-hand side of (4.45) is nothing but the following conditional expectation :

$$\frac{\partial \ln(p(\mathbf{y}; \boldsymbol{\alpha}))}{\partial \alpha_i} = \text{E}_{\mathbf{c}|\mathbf{y}} \left\{ \frac{\partial \ln(p(\mathbf{y} | \mathbf{x} = \mathbf{c}_i))}{\partial \alpha_i} \right\}. \quad (4.48)$$

Then, since the received samples are assumed to be independent, it follows from (4.48) that :

$$\frac{\partial \ln(p(\mathbf{y}; \boldsymbol{\alpha}^{(1)}))}{\partial S} = \sum_{k=0}^{K-1} \mathbb{E}_{c_k|\mathbf{y}} \left\{ -\frac{S|c_{i,k}|^2}{\sigma^2} + \frac{\Re(y^*(k)c_{i,k}S_{\phi,\vartheta})}{S\sigma^2} \right\} \quad (4.49)$$

$$\frac{\partial \ln(p(\mathbf{y}; \boldsymbol{\alpha}^{(1)}))}{\partial \sigma^2} = -\frac{1}{\sigma^2} + \sum_{k=0}^{K-1} \mathbb{E}_{c_k|\mathbf{y}} \left\{ \frac{|y(k) - c_{i,k}S_{\phi,\vartheta}|^2}{2\sigma^4} \right\}. \quad (4.50)$$

$$\frac{\partial \ln(p(\mathbf{y}; \boldsymbol{\alpha}^{(2)}))}{\partial \phi} = \sum_{k=k_0}^{k_0+K-1} \mathbb{E}_{c_k|\mathbf{y}} \frac{\Im(y^*(k)c_{i,k}S_{\phi,\vartheta})}{\sigma^2} \quad (4.51)$$

$$\frac{\partial \ln(p(\mathbf{y}; \boldsymbol{\alpha}^{(2)}))}{\partial \vartheta} = 2\pi k \sum_{k=k_0}^{k_0+K-1} \mathbb{E}_{c_k|\mathbf{y}} \frac{\Im(y^*(k)c_{i,k}S_{\phi,\vartheta})}{\sigma^2}, \quad (4.52)$$

The last expectations are computed empirically using the marginal APPs provided by the decoder. In fact, in turbo-coded systems, these marginal APPs are computed iteratively through the BCJR algorithms in the two SISO decoders, with exchange of extrinsic information at each iteration. When the coded bits (conditioned on \mathbf{y}) can be considered as independent (which is again a reasonable assumption due to the large-size interleaver) this iterative procedure yields the correct marginal APPs at the steady state [26]. To evaluate the FIM elements, however,

the expectation involved in (4.43) is performed through extensive Monte-Carlo simulations by generating a sufficiently large number of noise samples. The statistical expectation is then approximated by an arithmetic mean using all the generated realizations, according to the following formula :

$$\mathbb{E}\{f(X)\} = \frac{1}{L} \sum_{l=1}^L f(x(l)). \quad (4.53)$$

Chapitre 5

Simulation Results

5.1 SNR estimation

In this section, we provide graphical representations of the newly derived SNR CRLBs, for different modulation orders and different coding rates. The encoder is composed of two identical RSCs — with systematic rate $R = 1/2$ — which are concatenated in parallel. Their generator polynomials are $(1,0,1,1)$ and $(1,1,0,1)$. A large-size interleaver is placed between the two RSCs. The output of the turbo encoder is punctured in order to achieve the desired rates. For the tailing bits, the size of the RSC encoders memory is fixed to 4. First, we begin by comparing the analytical CRLBs to their empirical counterparts in Fig. 5.1. It is clearly seen from this figure

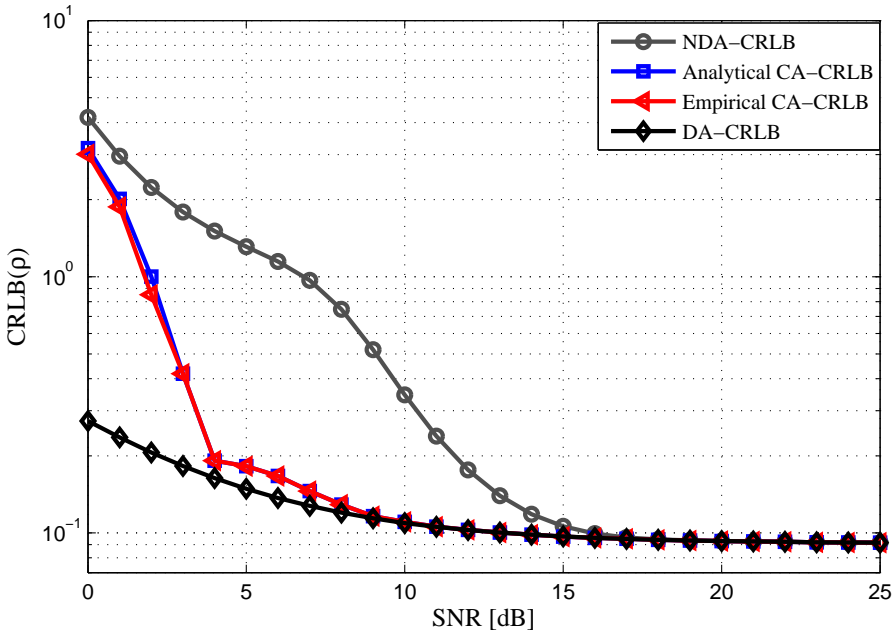


FIGURE 5.1 – CA CRLBs for SNR estimation : 16-QAM, $K=207$.

that the two CRLBs are exactly the same validating thereby our new analytical expressions. Therefore in the next figures we will plot the analytical CRLBs only. We also see from Fig. 5.1 that the CRLB for code-aided estimation is smaller than the CRLB for the NDA scenario. This highlights the estimation performance gain brought by leveraging the information about the transmitted bits that is delivered during the decoding process. This is to be opposed to the traditional NDA scheme where the SNR is estimated directly from the output of the matched filter. For instance, at the typical value of the SNR, $\rho = 4$ dB, the CA-CRLB is 10 times smaller than the NDA-CRLB. In addition, starting from relatively small SNR values (as low as $\rho = 4$

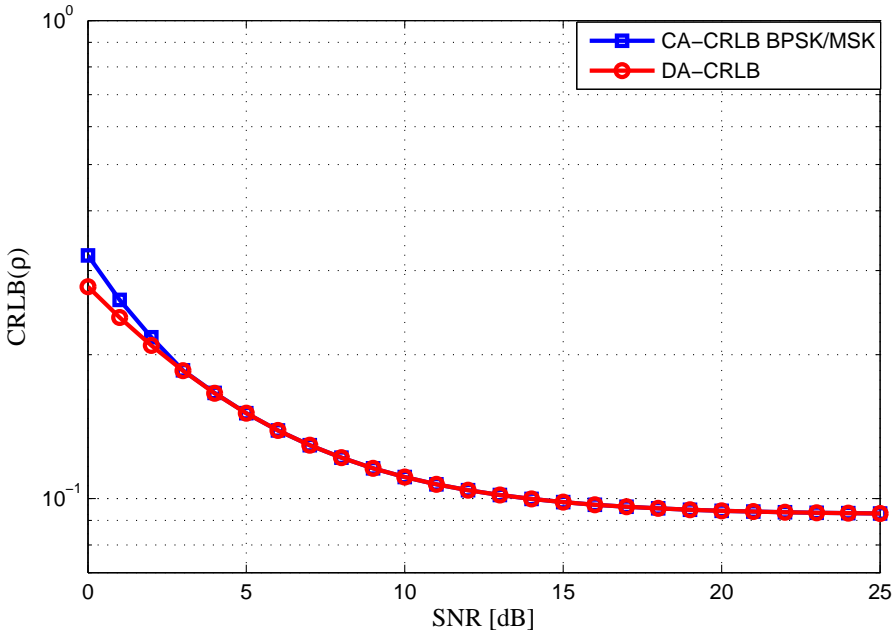


FIGURE 5.2 – CA CRLBs for SNR estimation : BSK and MSK signals, $K=207$.

dB), the CA CRLB reaches the DA CRLB which is simply given by [21] :

$$\text{CRLB}_{DA}(\rho) = \frac{100}{K \ln^2(10)} \left(1 + \frac{2}{\rho} \right). \quad (5.1)$$

Recall that the DA CRLB is associated to an ideal case where all the bits (or equivalently the symbols) are perfectly known. Therefore, even without relying on any pilot sequence, code-aware estimation is equivalent to DA estimation over a wide range of practical SNRs.

In Figs. 5.2 and 5.3, we plot the CA CRLB for BPSK-/MSK- and square-QAM-modulated signals (with different orders), respectively.

In Fig. 5.2, it is seen that for BPSK and MSK signals, the gap between the NDA and DA

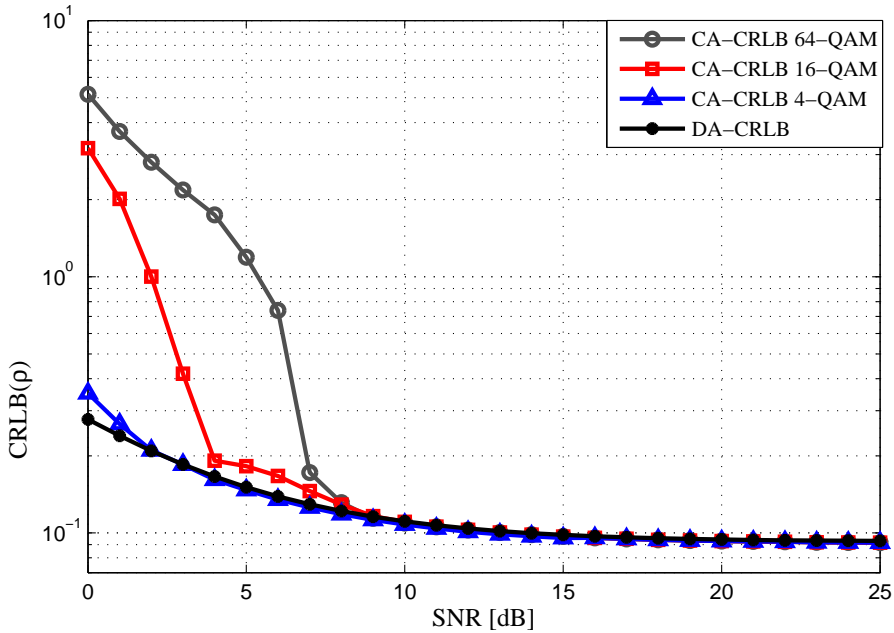


FIGURE 5.3 – CA CRLBs with different modulation orders : $K = 207$.

CRLBs can be totally bridged by relying on code-aided estimation. From Fig. 5.3, however, it is seen that this gap increases as the modulation order increases. Yet, the CA CRLBs still reach the DA CRLB at relatively small SNR values contrarily to the NDA CRLBs as shown in Fig. 5 of [22]. Fig. 5 depicts the effect of the coding rate on the SNR estimation performance. Two coding rates of $R_1 = 0.3285 \approx \frac{1}{3}$ and $R_2 = 0.4892 \approx \frac{1}{2}$ are considered. Even though the corresponding CA CRLBs ultimately coincide at moderate SNR levels, they exhibit a significant gap at lower SNR values. In fact, with smaller coding rates, more redundancy is provided by the turbo encoder and the bits can be decoded more accurately. In this case, the *extrinsic* information, which is used to approximate the LLRs [8, 25], is increasingly high (in absolute

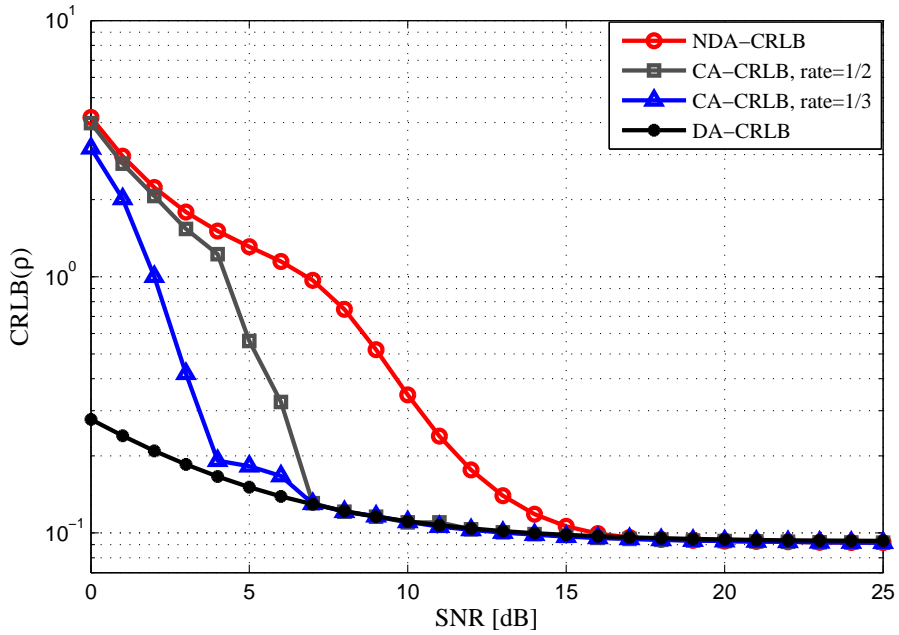


FIGURE 5.4 – CA CRLBs for different coding rates : 16-QAM, $K=207$.

value) and CA estimation resembles much more to DA estimation.

5.2 Phase and CFO estimation

In this section, we provide graphical representations of the newly derived closed-form CRLBs for the joint estimation of parameters ϕ and ϑ , with different modulation orders and different coding rates. We use the same setup as to the CRLB for the SNR simulations. Here we mention that the FIM associated with the parameters ϕ and ϑ depends on the time index k_0 . Consequently, we obtain different loose bounds as k_0 varies. This is not the case for the SNR estimation,

in which k_0 is irrelevant to the CRLB obtained. Our interest is focused on the tightest bound, which is ideally obtained if the two parameters are decoupled, i.e., the square of the off-diagonal elements is negligible compared to the product of the diagonal ones :

$$[\mathbf{I}(\boldsymbol{\alpha}^{(2)})]_{1,2}^2 \ll [\mathbf{I}(\boldsymbol{\alpha}^{(2)})]_{1,1}[I(\boldsymbol{\alpha}^{(2)})]_{2,2}. \quad (5.2)$$

Hence, the best performance is obtained when we choose k_0 in the middle of the observation interval, i.e., $k_0 = -\frac{K-1}{2}$. The off-diagonal terms of the FIM are identical to zero in case of NDA estimation.

In Fig. 5.5, we verify that the new closed-form CRLBs, derived in this paper, coincides with their empirical counterpart earlier obtained earlier in [28]. This means that the new analytical expressions corroborate previous attempts to evaluate the considered bounds and they allow their immediate evaluation for any square-QAM turbo-coded signal.

We also see from the same figure that, as expected, the CRLB for code-aided estimation is smaller than the CRLB for the NDA estimation. This highlights the performance improvements that can be achieved by a coded system compared to an uncoded one. For example, in Fig. 5.5.a, at $SNR = 4$ dB, the code-aided CRLB is 10 times smaller than the NDA-CRLB. Additionally, we observe that even at relatively small SNR levels the CA CRLB coincides with the DA CRLB,

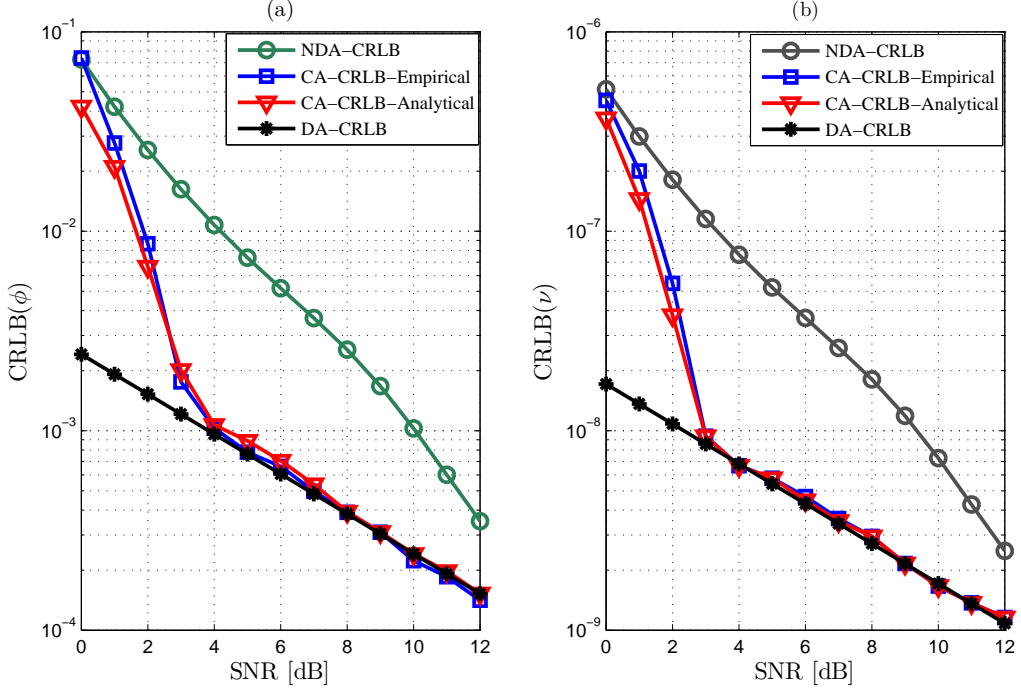


FIGURE 5.5 – CRLB for the phase and CFO estimation using 16-QAM symbols with $K = 207$:

(a) $\text{CRLB}(\phi)$, (b) $\text{CRLB}(\nu)$

which is given by the following expressions :

$$\text{MCRLB}(\nu) = \frac{6}{(2\pi)^2 K(K^2 - 1)\rho}, \quad (5.3)$$

$$\text{MCRLB}(\phi) = \frac{1}{2K\rho}, \quad (5.4)$$

$$(5.5)$$

In Figs. 5.6 and 5.7, we plot the CA-CRLB for different modulation types.

It is clear that the CRLB increases with the modulation order at a fixed SNR value. In Fig.

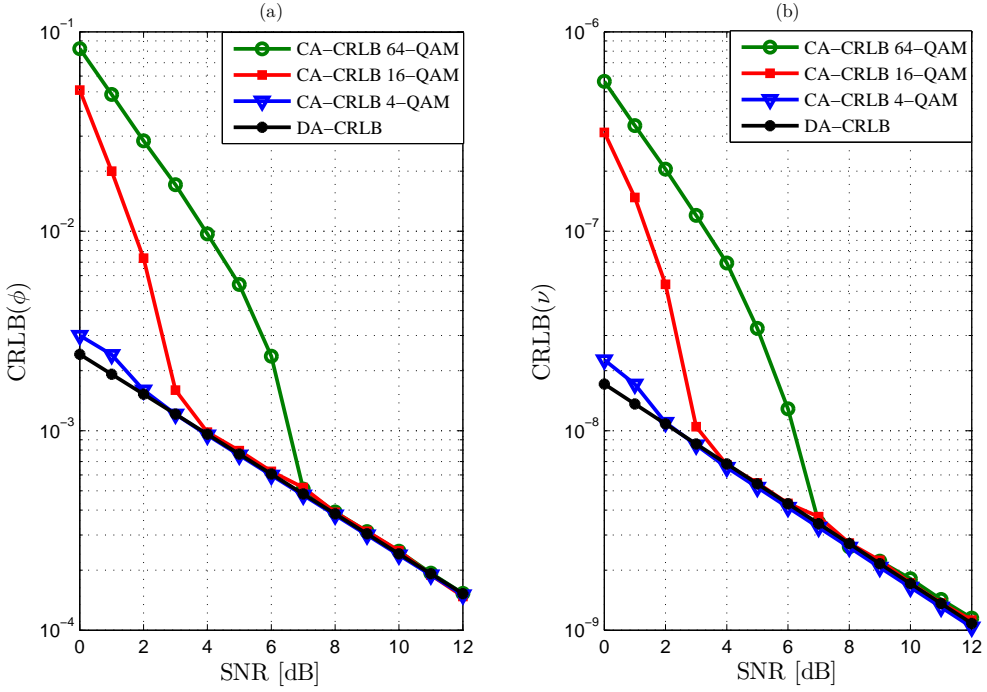


FIGURE 5.6 – CRLB for the phase and CFO estimation for different modulation orders with $K=207$ symbols : (a)- $\text{CRLB}(\phi)$,(b)- $\text{CRLB}(\nu)$

5.8, we show the effect of the coding rate on the synchronization performance. In fact, we plot the CRLB for the carrier phase estimation using two different coding rates $R_1 = 0.3285 \approx \frac{1}{3}$ and $R_2 = 0.4892 \approx \frac{1}{2}$. Even though both CRLBs coincide at moderate SNRs, they exhibit a significant gap at lower SNR values. In fact, with smaller coding rates, more redundancy is provided by the turbo encoder and better estimation performance can be achieved.

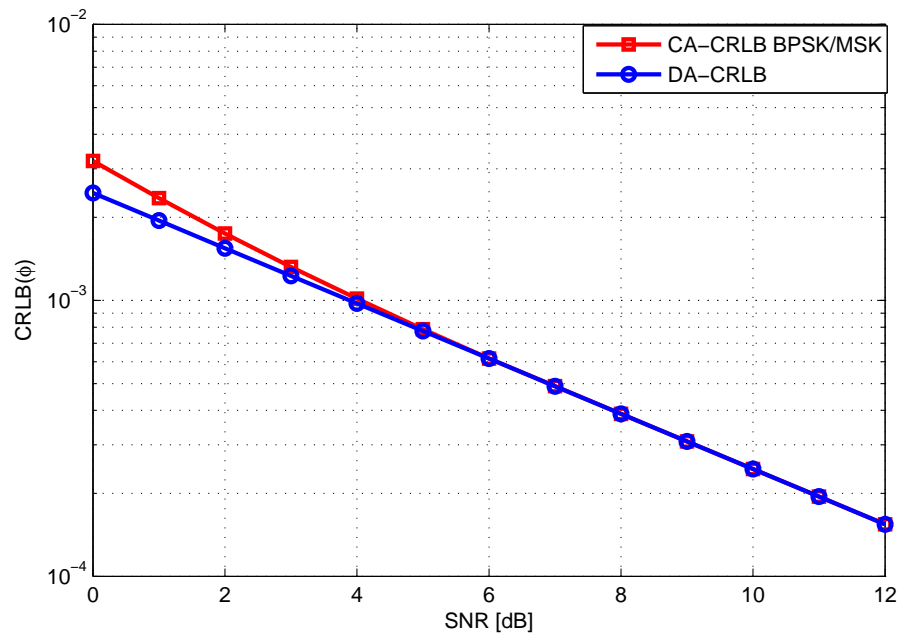


FIGURE 5.7 – CRLB for the phase estimation for BPSK and MSK modulations $K=207$ symbols :

$$\text{CRLB}(\phi)$$

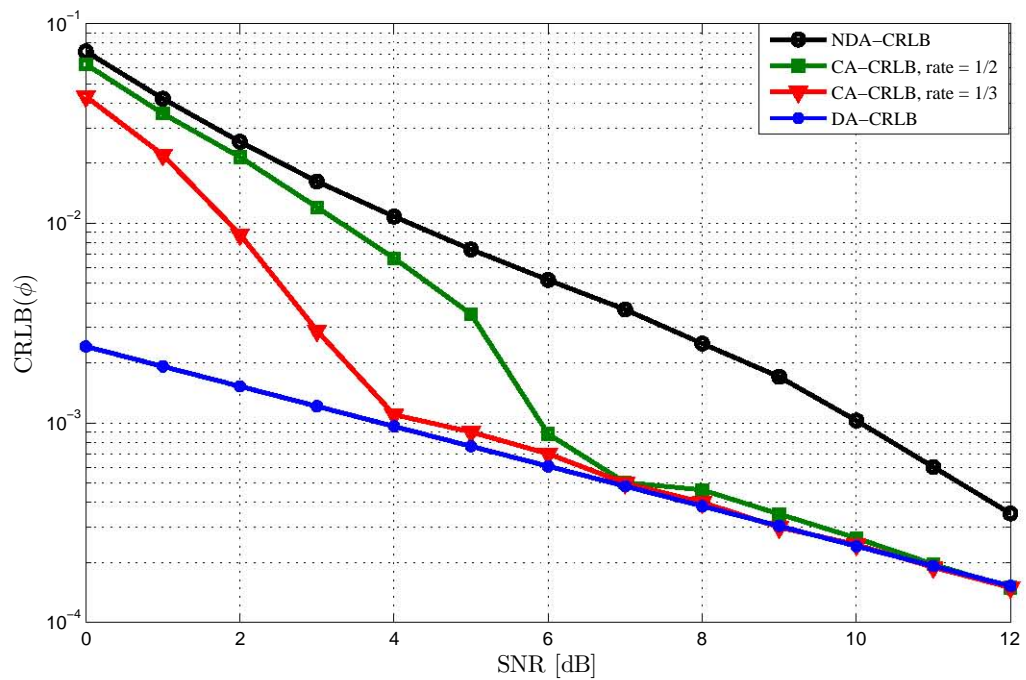


FIGURE 5.8 – CRLB for the phase : $CRLB(\phi)$ vs coding gain, for 16-QAM symbols, $K=207$.

Chapitre 6

Conclusion

In this report, we tackled the problem of deriving analytical expressions for the Cramer-Rao bounds for coded wireless communication systems, in the case of BPSK, MSK and square QAM modulated signals, for SNR, channel phase and CFO. We were able to derive for the first time closed-form expression of the CRB for the estimation of these parameters, in the case of BPSK , MSK and quare QAM modulations (except for the case of BPSK for SNR estimation, which exists already). Our newly derived CRBs corroborate previously obtained empirical CRBs and are hence validated. We found that these CRBs are always smaller than the NDA CRBs which reflects the advantage of coding in enhancing the estimation of the considered parameters, especially in the average and low SNR range. The CRBs in the case of

BPSK and MSK modulations coincide. We also studied the effect of the coding rate on the CRBs and found that the less the coding rate, implying more redundancy on the coding process, the smaller the CRBs get, which implies a better performance in the code aided estimation.

Bibliographie

- [1] S. Nanda, K. Balachandran and S. Kumar, “Adaptation techniques in wireless packet data services,” *IEEE Trans. Commun.*, vol. 38, pp. 54-64, 2000.
- [2] S. Talakoub and B. Shahrrava, “Turbo Equalization with Integrated SNR Estimation,” *IEEE GlobeCom*, San Francisco, CA, pp. 1-5, Nov. to Dec. 2006.
- [3] S. Talakoub and B. Shahrrava, “Turbo equalization with iterative online SNR estimation,” in *Proc. IEEE Wireless Communications and Networking Conference*, New Orleans, vol. 2, pp. 1097-1102, March 2005.
- [4] J. G. Proakis, *Digital Communications*, 2001 :McGraw-Hill
- [5] K. Balachandran, S. R. Kadaba and S. Nanda, “Channel quality estimation and rate adaptation for cellular mobile radio,” *IEEE J. Sel. Areas Commun.*, vol. 17, pp. 1244-1256, 1999.

- [6] C. Berrou and A. Glavieux, “Near optimum error correcting coding and decoding : turbo codes,” *IEEE Trans. Commun.* , vol. 44, no. 10, pp. 1261-1271, Oct. 1996.
- [7] J. Hagenauer, “The turbo principle : tutorial introduction and state of the art,” *in Proc. Int. Symp. on Turbo Codes and Related Topics.*, Brest, France, pp. 1-11, Sept. 1997.
- [8] G. Colavolpe, G. Ferrari and R. Raheli, “Extrinsic information in iterative decoding : A unified view,” *IEEE Trans. Commun.*, vol. 49, pp. 2088-2094, 2001.
- [9] M. A. Dangl and J. Lindner, “How to use a priori information of data symbols for SNR estimation,” *IEEE Signal Process. Lett.*, vol. 13, pp. 661-664, Nov. 2006.
- [10] N. Wu, H. Wang and J.M. Kuang, “Code-aided SNR estimation based on expectation maximisation algorithm,” *Electron. Lett.*, vol. 44, pp. 924-925, July 2008.
- [11] N. Wu, H. Wang and J M. Kuang, “Maximum likelihood signal-to-noise ratio estimation for coded linearly modulated signals,” *IET Commun.*, vol. 4, pp. 265-271, 2010.
- [12] M. Bergmann, W. Gappmair, H. Schlemmer and O. Koudelka, “Code-aware joint estimation of carrier phase and SNR for linear modulation schemes,” *in Proc. 5th Advanced Satellite Multimedia Systems Conference*, Cagliari/Italy, pp. 177-182, Sept. 2010.
- [13] L.Bahl, J.Cocke, F.Jelinek and J.Raviv, “Optimal Decoding of Linear Codes for minimizing symbol error rate,” *IEEE Transactions on Information Theory*, vol. IT-20(2), pp.284-287,

March 1974.

- [14] M.A. Khalighi, "Effect of Mismatched SNR on the performance of log-MAP turbo detector," *IEEE Trans on Vehic. Tech.*, vol. 52, no. 5, pp. 1386-1397, Sept. 2003.
- [15] K.T. Shr and Y.H. Huang, "SNR estimation based on metric normalization frequency in Viterbi decoder," *IEEE Commun. Lett.*, vol. 15, no. 6, pp. 668-670, June 2011.
- [16] T. A. Summers and S. G. Wilson, "SNR mismatch and online estimation in turbo decoding," *IEEE Trans. Commun.*, vol. 46, pp.421-423, 1998.
- [17] M. C. Reed and I. Asenstorfer, "A novel variance estimator for turbocode decoding," in *Proc. Int. Conf. Telecommunications*, Melbourne, Australia, pp. 173-178, Apr. 1997.
- [18] A. Worm, P. Hoeher and N. Web, "Turbo-decoding without SNR estimation," *IEEE Commun. Lett.*, vol. 4, no. 6, pp. 193-195, 2000.
- [19] S. L. Goff, A. Glavierw and C. Berrou, "Turbo-codes and high spectral efficiency modulation," in *Proc. ICC'94.*, New Orleans, LA, pp. 645-649, May 1994.
- [20] S. Minying, L. Yuan and S. Sumei, "Impact of SNR estimation error on turbo code with high-order modulation," *IEEE VTC Spring*, vol. 3, pp. 1320-1324, May 2004.
- [21] N. S. Alagha, "Cramèr-Rao bounds of SNR estimates for BPSK and QPSK modulated signals," *IEEE Commun. Lett.*, vol. 5, pp.10-12, 2001.

- [22] F. Bellili, A. Stèphenne and S. Affes, “Cramèr-Rao bounds for NDA SNR estimates of square QAM modulated signals,” *Proc. IEEE Wireless Commun. Netw. Conf. (WCNC)*, 2009.
- [23] F. Bellili, A. Stèphenne and S. Affes, “Cramèr-Rao lower bounds for non-data-aided SNR estimates of square QAM modulated transmissions,” *IEEE Trans. Commun.*, vol. 58, pp. 3211-3218, 2010.
- [24] V. Lottici and M. Luise, “Embedding carrier phase recovery into iterative decoding of turbo-coded linear modulations,” *IEEE Trans. Commun.*, vol. 52, no. 4, pp. 661-669, April 2004.
- [25] L. Zhang and A. Burr, “Iterative carrier phase recovery suited for turbo-coded systems,” *IEEE Trans. Wireless Commun.*, vol. 3, no. 6, pp. 2267-2276, 2004.
- [26] T. Richardson, “The geometry of turbo-decoding dynamics,” *IEEE Trans. Inf. Theory*, vol. 46, pp. 9-23, Jan 2000.
- [27] S. M. Kay, *Fundamentals of Statistical Signal Processing-Detection Theory*. Englewood Cliffs, NJ : Prentice-Hall, 1998.
- [28] N. Noels, H. Steendam and M. Moeneclaey, “The Cramér-Rao bound for phase estimation from coded linearly modulated signals,” *IEEE Commun. Lett.* , vol. 7, no. 5, pp. 207-209,

May 2003.

- [29] A. Anastasopoulos and K. M. Chugg, “Adaptive iterative detection for phase tracking in turbo-coded systems,” *IEEE Trans. Commun.*, vol. 49, no. 12, pp. 2135-2144, Dec. 2001.
- [30] B. Mielczarek and A. Svensson, “Phase offset estimation using enhanced turbo decoders,” in *Proc. IEEE Int. Conf. Commun. (ICC '02)*, New York, NY, USA, vol. 3, pp. 1536-1540, April 2002.
- [31] N. Wiberg, “Simultaneous decoding and phase synchronization using iterative \tilde{S} turbo \tilde{T} decoding,” in *IEEE Int. Symp. Information Theory*, Ulm, Germany, pp. 11, June 29-July 4, 1997.
- [32] C. Komninakis and R. D. Wesel, “Joint iterative channel estimation and decoding in flat correlated rayleigh fading,” *IEEE J. Sel. Areas Commun.*, vol. 19, pp. 1706-1717, Sept. 2001.
- [33] C. Morlet, I. Buret and M.-L. Boucheret, “A carrier phase estimator for multi-media satellite payloads suited to RSC coding schemes,” in *IEEE Int. Conf. Commun.*, New Orleans, LA, vol. 1, pp. 455-459, 2000.
- [34] C. Langlais and M. Helard, “Phase carrier for turbo codes over a satellite link with the help of tentative decisions,” in *Int. Symp. Turbo Codes Related Topics*, vol. 5, pp. 439-442,

2000.

- [35] S. Cioni, G. E. Corazza and A. Vanelli-Coralli “Turbo embedded estimation with imperfect phase/frequency recovery,” *Proc. IEEE Int. Conf. Commun.*, vol. 4, pp.2385-2389, May 2003.
- [36] W. Oh and K. Cheun, “Joint decoding and carrier phase recovery algorithm for turbo codes,” *IEEE Commun. Lett.*, vol. 5, pp. 375-377, Sept. 2001.
- [37] N. Noels, C. Herzet, A. Dejonghe et al. : “Turbo-synchronization : an EM algorithm approach,” *Proc. IEEE ICC*, pp. 2933-2937, 2003.
- [38] X. Wu, Y. Song, C. Zhao and X. You, “Progressive frequency offset compensation in turbo receivers,” *IEEE Trans. Wirel. Commun.*, vol. 10, no. 2, pp. 702-709, 2011.
- [39] Herzet, C. : “Code-aided synchronization for digital burst communications.” PhD dissertation, Communications Laboratory, University catholique de Louvain, 2006.
- [40] B. Cowley, F. Rice, and M. Rice, “Cramér-Rao lower bound for QAM phase and frequency estimation,” *IEEE Trans. Commun.*, vol. 49, no. 9, pp. 689-693, Sept. 2001.
- [41] F. Bellili, N. Atitallah, S. Affes and A. Stéphenne, “Cramér-Rao lower bounds for frequency and phase NDA estimation from arbitrary square QAM-modulated signals,” *IEEE Trans. Signal Process.*, vol. 58, pp. 4517-4525, Sept. 2010.

- [42] N. Noels, H. Steendam and M. Moeneclaey, “Carrier and Clock recovery in (turbo) coded systems : Cramér-Rao bound and synchronizer performance,” *EURASIP Journal on App. Signal process., Special Issue on Turbo Processing*, vol. 2005, no. 6, pp. 972-980, May 2005.
- [43] F. Bellili, A. Methenni and S. Affes, “Closed-Form CRLBs for SNR Estimation from Turbo-Coded BPSK-, MSK- and Square-QAM-Modulated Signals,” *IEEE Trans. Signal Process.*, submitted.
- [44] F. Bellili, A. Methenni and S. Affes, “Closed-Form CRLBs for CFO and Phase Estimation from Turbo-Coded BPSK-, MSK- and Square-QAM-Modulated Signals,” *IEEE Wirel. Comm. ,* submitted.
- [45] A. Methenni, F. Bellili, S. Affes and A. Stéphenne, “Stochastic NDA CRLB for DOA estimation over SIMO systems,” *Proc. of IEEE VTC’2012-Spring*, Yokohama, Japan, May 6-9, 2012.